SGSMP
SSRPM
SSRFM

Schweizerische Gesellschaft für Strahlenbiologie und Medizinische Physik
Société Suisse de Radiobiologie et de Physique Médicale
Società Svizzera di Radiobiologia e di Fisica Medica
Swiss Society of Radiobiology and Medical Physics

55th SSRMP Annual Meeting

27. – 28. October 2022

Kultur- und Kongresszentrum Thun

Booklet

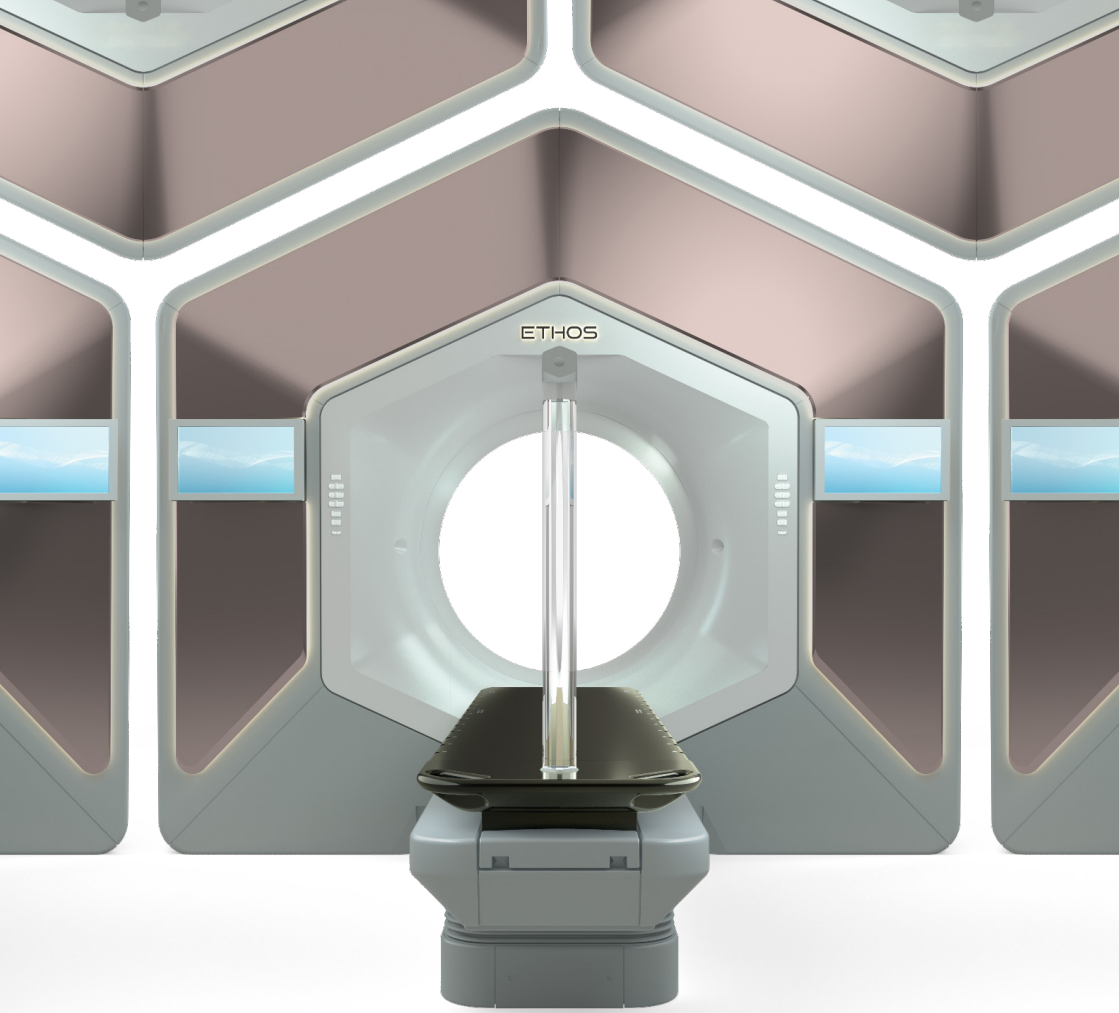

The more efficient, flexible, personal

& intelligent way to outsmart cancer.

With Ethos™ therapy, you can adapt treatment plans daily while transforming your cancer fight completely.

Ethos therapy is our AI-driven holistic solution that lets you choose the most appropriate treatment option based on daily changes in patient anatomy. It also delivers an entire adaptive treatment in a typical 15-minute timeslot, from setup through delivery. Redefine how you fight cancer—experience Ethos therapy at varian.com/ethos today.

Safety Information: Radiation may cause side effects and may not be appropriate for all cancers.

varian
A Siemens Healthineers Company

ETHOS™

SGSMP SSRPM SSRFM

THANKS to the Sponsors & Exhibitors

SGSMP SSRPM SSRFM

varian
A Siemens Healthineers Company

CONMEDICA
High End Radiotherapy

RADIO-ONKOLOGIE BERNER OBERLAND AG

spitalSTSAG

Elekta

SIEMENS Healthineers

SUN NUCLEAR

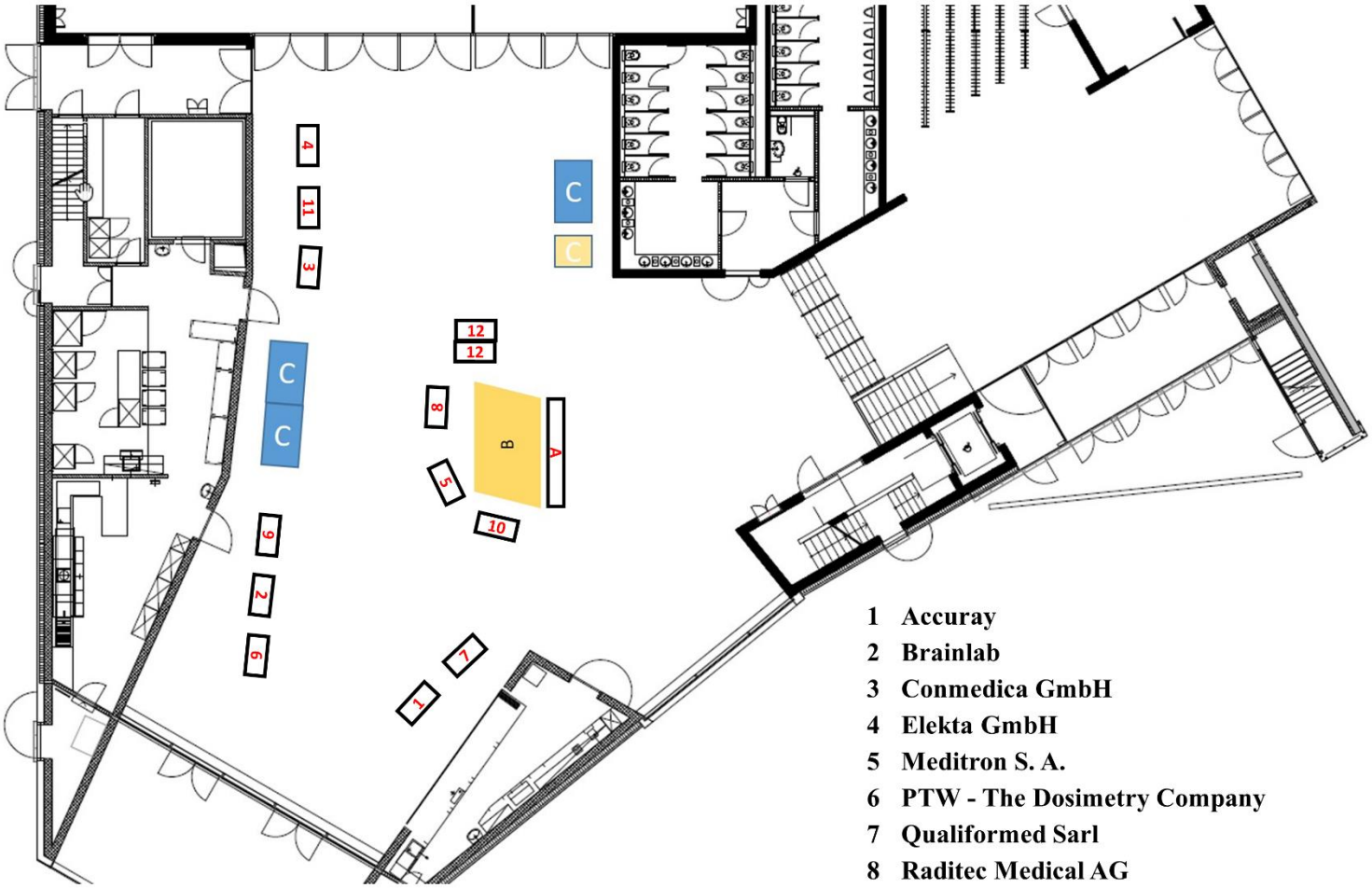

1 Accuray
2 Brainlab
3 Conmedica GmbH
4 Elekta GmbH
5 Meditron S. A.
6 PTW - The Dosimetry Company
7 Qualiformed Sarl
8 Raditec Medical AG
9 Siemens Healthcare AG
10 Solumedics AG
11 Sun Nuclear
12 Varian Medical Systems International AG
A Poster Area
B Goldbarren
C Catering

Meeting Program

Thursday, 27th October 2022

09:00 – 10:00	Registration
10:00 – 10:15	Opening
10:15 – 11:35	Session I: QA, Dosimetry, Treatment Planning Chair: Dr. Maud Jaccard
11:35 – 12:30	Poster & Industry
12:30 – 13:45	Lunch & Industry
13:45 – 15:15	Session II: Radiobiology, Radiomics, Adaptive RT Chair: Dr. Jenny Bertholet
15:15 – 15:45	Coffee Break & Industry
15:45 – 16:30	Invited Speaker: Dr. Markus Notter Hyperthermia as a radiosensitizer: the potential and evidence, some hurdles and pitfalls Chair: Dr. Silvan Mueller
16:30 – 18:00	SSRMP General Assembly 2022
19:00 – 22:00	Social Event

Friday, 28th October 2022

09:00 – 09:45	Invited Speakers: Dr. Thomas Götzfried, Dr. Thiago Lima Experiences from clinical audits in radiology, nuclear medicine and radiation oncology Chair: Dr. Silvan Mueller
09:45 – 10:15	Coffee Break & Industry
10:15 – 11:55	Session III: Imaging Chair: Dr. Lukas Wissmann
11:55 – 13:15	Lunch & Industry
13:15 – 14:45	Session IV: Radioprotection, Treatment Techniques Chair: Francesca Belosi
14:45 – 15:15	Coffee Break & Industry
15:15 – 16:00	Invited Speaker: Dr. Paola Ballesteros Zebadua Understanding the radiobiology of FLASH radiotherapy Chair: Dr. Silvan Mueller
16:00 – 16:15	Closing

Contributions

Poster presentations 27.10.2022		
	Dietmar Marder	Pilot studies using an ESHO quality assurance phantom for phased-array deep hyperthermia devices
	Diana Wüthrich	Study of the influence of optimisation parameters on the Pareto front for prostate cancer
	Amith Kamath	Evaluating a deep learning based 3D dose prediction model for quality assurance of organ at risk contours.

Session I: QA, Dosimetry, Treatment Planning 27.10.2022		
10:15 - 10:25	Michael Baumgartl	A comparison of two approaches for checking the source positioning accuracy in brachytherapy
10:25 - 10:35	Paul-Henry Mackeprang	Comparing dry-run and delivery modes for dynamic trajectory radiotherapy
10:35 - 10:45	Gian Guyer	Development of a collision prediction tool using Blender for non-coplanar radiotherapy on a C-arm linear accelerator
10:45 - 10:55	Valery Taranenko	CyberKnife preliminary commissioning model for a twinned beam
10:55 - 11:05	Carlos V. G. Ferreira	Calculation of dosimetric parameters in paediatric phantoms using Monte Carlo techniques for 18F-FDG and the new TIAC
11:05 - 11:15	Lisa S. Fankhauser	Assessing the robustness of normal tissue complication probability of head and neck treatment plans to contouring uncertainties
11:15 - 11:25	Michele Zeverino	Clinical implementation of machine learning autoplanning for breast treatments: the CHUV recipe
11:25 - 11:35	Hannes A. Loebner	Development of a lexicographic automatic intensity optimization process

Session II: Radiobiology, Radiomics, Adaptive RT 27.10.2022		
13:45 - 13:55	Evangelia Choulilitsa	Dose guidance in daily adaptive proton therapy: Predicting the cumulative treatment dose
13:55 - 14:05	Daniel Schmidhalter	Dosimetric accuracy verification of treatment plans generated during online adaptive radiotherapy
14:05 - 14:15	Lusine Hovhannisyan	MET-targeting CAR T cells enhance tumor cell killing and cytokines release in glioma models when combined with radiation therapy
14:15 - 14:25	Lusine Hovhannisyan	Fractionated radiation therapy increases Siglec-7 and -9 ligands expression in cancer cells
14:25 - 14:35	Lars Widmer	Influence of image resolution and extraction software on the stability of radiomic features
14:35 - 14:45	Zahra Khodabakhshi	Magnetic resonance imaging radiomic features stability in brain metastases
14:45 - 14:55	Hubert Gabrys	PET/CT radiomics for prediction of hyperprogression in metastatic melanoma patients treated with immune checkpoint inhibitors
14:55 - 15:05	Hannes A. Loebner	Feasibility and mechanical accuracy of gated dynamic trajectory radiotherapy
15:05 - 15:15	Sergejs Popovs	Influence of two-level quality assurance methodology on safety margins size and planning target volumes in frameless mask-based image-guided stereotactic intracranial radiosurgery and radiotherapy.

Session III: Imaging 28.10.2022		
10:15 - 10:25	Alisha Duetschler	Towards more realistic 4DCT(MRI) numerical lung phantoms
10:25 - 10:35	Damien Racine	New methodology to assess spatiotemporal image quality on fluoroscopy devices
10:35 - 10:45	Hannah J. Eggimann	Fluoroscopy-guided intervention for a splenic artery aneurysm during pregnancy: Evaluation and optimization of fetal radiation exposure
10:45 - 10:55	Lucia G. Manzano	Clinical commissioning of the MARS spectral photon-counting CT and its first clinical application for the diagnosis of crystal arthropathies
10:55 - 11:05	Javier B. Garcia	Self-supervised skin lesion screening in dermatology consultation
11:05 - 11:15	Milena C. Gravinatti	Comparison of mammography image quality across different radiology departments based on the IAEA technical report on the Implementation of an Automated Quality Control Programme.
11:15 - 11:25	Philipp Wallimann	N-Peaks, a novel method of intensity normalization for magnetic resonance images
11:25 - 11:35	Song Xue	Practice of domain knowledge towards robust and generalizable deep learning-based CT-free PET attenuation and scatter correction
11:35 - 11:45	Mariia Lapaeva	Comparison of generative adversarial networks trained in paired and unpaired fashion for MR-based synthetic CT generation towards MR-only radiotherapy in the abdomen
11:45 - 11:55	Thiago Lima	Dosimetric and image quality comparison of radiation oncology and radiology head scan protocols

Session IV: Radioprotection, Treatment Techniques 28.10.2022		
13:15 - 13:25	Chengchen Zhu	Dosimetrically-motivated beam-angle optimization for partial-arc non-coplanar VMAT
13:25 - 13:35	Reto Treier	Involvement of medical physicists in medical practices operating a fluoroscopy system
13:35 - 13:45	Barbara Ott	Monitoring of medical population dose in Switzerland – How to move forward
13:45 - 13:55	Laura Dupont	Proposed DRLs for mammography in Switzerland
13:55 - 14:05	Marion Dercourt	Kerma - effective dose factor of the eye of pediatric patient during intra-arterial chemotherapy
14:05 - 14:15	Silvan Mueller	On an auto-commissioning for an electron beam model applicable to MLC collimated electron beams
14:15 - 14:25	Anne H. zur Horst	Dosimetric comparison between modulated electron radiotherapy, mixed beam radiotherapy and volumetric modulated arc therapy
14:25 - 14:35	Florian Amstutz	Role of proton beam angle flexibility for combined proton-photon therapy of head and neck cancer
14:35 - 14:45	Vivek Maradia	An ultra-fast field delivery with PSI's Gantry-2 to achieve hypofractionated PBS proton therapy within a single breath-hold for lung cancer

Poster presentations

27.10.2022, 11:35 – 12:30

Pilot studies using an ESHO quality assurance phantom for phased-array deep hyperthermia devices

Author: Dietmar Marder[1,2]

Co-authors: Adela Ademaj[1], Olaf Timm[1], Emsad Puric[1], Hana Dobšíček Trefná[2], Gerard van Rhoon[2], Manfred Schmidt[2], Ulf Lamprecht[2], Jacek Nadobny[2], Sultan Abdel-Rahman[2], Marianne Gröger-Neff[2], Hans Crezee[2], Petra Kok[2], Dario B. Rodrigues[2], Sergio Curto[2], Remko Zweije[2], Mattia de Lazzari[2], Oliver Riesterer[1]

[1]*Kantonsspital Aarau, Radio-Onkologie-Zentrum KSA-KSB, Aarau, Switzerland*

[2]*ESHO technical committee*

Purpose

Phantoms for quality assurance (QA) of deep hyperthermia therapy (DHT) devices are not commercially available. In this work, we suggest an easy to build phantom to perform commissioning and regular QA on the performance of DHT phased-array devices.

Materials and Methods

The phantom container consists of a 64cm long polyurethane tube with an external diameter of 25cm and a wall thickness of 8 mm, where both ends are sealed with discs. Inside the tube, 3D-printed structures hold 13 catheters spaced by 3 cm and distributed in a cross shape.The central catheter is extended to cover the full length of the container. The phantom is filled with a tissue-equivalent gel. After placing the phantom in the BSD-2000 3D Sigma Eye applicator (Pyrexar Medical, Salt Lake City, USA), a power pulse of 1000W for 10 minutes at 100MHz is applied, with equal amplitudes and phase settings to target the center of the phantom. Temperature is recorded inside the catheters using thermistors provided with the BSD-2000 3D system. A scanning method with a 5mm step is performed for the longitudinal axis measurement. From the longitudinal data, the position of the center and the extension (full width at half maximum, FWHM) of the heated volume is determined.

Results

A maximum temperature rise of $\Delta T=7.6°C$ was measured at the center of the phantom after the 10 minutes power pulse. Along the longitudinal axis, a high-resolution profile is achieved over a length of 60cm. From the longitudinal data the position of the center and the extension (full width at half maximum – FWHM = 32.5cm) of the heated volume can be determined. In the vertical and horizontal directions, only the position of the center is clearly defined by fitting a polynomial curve.

Conclusion

The proposed phantom allows the commissioning of new devices and regular QA measurements for DHT phased-array systems. Fast temperature rise measurements can be used to determine the FWHM in the longitudinal direction and the center of the heating focus in all three spatial directions.

Study of the influence of optimisation parameters on the Pareto front for prostate cancer

Author: Diana Wüthrich[1,2]

Co-authors: Michele Zeverino[1], Jean Bourhis[3], François Bochud[1], Raphaël Moeckli[1]

[1]*Institute of Radiation Physics, Lausanne University Hospital, Lausanne, Switzerland*

[2]*University of Lausanne, Lausanne, Switzerland*

[3]*Department of Radiation Oncology, Lausanne University Hospital, Lausanne Switzerland*

Purpose

To study the influence of objective functions and weights, as well as mean doses to secondary organs at risk (OAR) on Pareto front robustness.

Materials and Methods

We wrote and validated a python script that controls RayStation (RaySearch) treatment planning system (TPS) and calculates Pareto fronts. Then, we randomly chose thirty-one prostate cancer patients treated at our clinic and generated reference Pareto fronts for each of those patients for a given set of objective functions and weights. Hereby, we varied the planned target volume (PTV) coverage and rectum mean dose, and blocked the bladder and femoral heads mean doses. Afterwards, we calculated Pareto fronts for each patient using different optimisation parameters, and compared those fronts to the reference Pareto fronts using a validated metric (clinical distance)[1].

Results

The in-house script calculates a good approximation of the Pareto front. The relative PTV-rectum-overlap volume correlates with the clinical distance of those Pareto fronts. The Pareto fronts are different for different optimisation parameters. Hereby, the parameters most influencing the front and leading to clinically significant differences are the dose gradient around the PTV, the weight of the PTV objective function and the mean dose to the bladder.

Conclusion

We found out which anatomic trait and which optimisation parameters most affect the position of the Pareto front and gained insights into the interplay between the rectum and bladder mean dose optimisation criteria.

References

[1] Petersson K, Kyroudi A, Bourhis J, et al. A clinical distance measure for evaluating treatment plan quality difference with Pareto fronts in radiotherapy. Physics and Imaging in Radiation Oncology. 2017;3:53–56. https://doi.org/10.1016/j.phro.2017.09.003

Evaluating a deep learning based 3D dose prediction model for quality assurance of organ at risk contours

Author: Amith Kamath[1]

Co-authors: Robert Poel[1], Mauricio Reyes[1]

[1]*ARTORG Center for Biomedical Research, University of Bern, Bern, Switzerland*

Purpose

One of the recent methods to improve the efficiency, consistency and overall plan quality in radiotherapy is to use dose prediction. Based on prior experience of similar cases, deep neural networks can predict an achievable dose for a specific case. Instead of planning purposes, we are exploring the possibilities of using dose prediction in the QA of automatic segmentation. For this, we made a dose prediction model for the volumetric modulated arc therapy (VMAT) treatment of glioblastoma.

Materials and Methods

The data of 100 glioblastoma cases who received treatment at the InselSpital was collected. For all cases a VMAT plan was constructed according to a strict clinical dose prescription template. The resulting 100 dose distributions, the contours of the OARs and PTV and the planning CT were used to train the model. Training was performed in 3D on the OpenKPB dose prediction model [1]. Sixty cases were used for training and 20 cases each were used for validation and testing. The results of the predictions were compared with the reference plans on both the 3D dose score and the DVH score [1].

Results

The predictions of the test set had an overall 3D dose score of 0.906 ± 0.01 and a DVH score of 1.943 ± 0.04 , compared to the reference plans. The worst results in the test set upon close examination where caused by irregular shaped targets that defy the physical limitation of the delivery technique, OARs overlapping with the target or planning inconsistencies of the reference plan.

Conclusion

With a carefully curated training set, the OpenKBP dose prediction model provides good predictions for VMAT glioblastoma treatment according to the clinical protocol that was used. Our next steps will be improve the training set to make predictions more robust to a broad range of scenarios.

Session I: QA, Dosimetry, Treatment Planning

27.10.2022, 10:15 – 11:35

Chair: Dr. Maud Jaccard,

Service de Radio-Oncologie Clinique de Genolier

A comparison of two approaches for checking the source positioning accuracy in brachytherapy

Author: Michael Baumgartl[1]

Co-authors: Nikolaus Kremer[1], Stephanie Tanadini-Lang[1], Klara Uher[1]

[1]*Department of Radiation Oncology, University Hospital Zurich, Zurich, Switzerland*

Purpose

In brachytherapy remote afterloaders are used to transfer a radioactive source via transfer tubes to applicators or interstitial needles with submillimetre accuracy. Predefined dwell positions and dwell times of the source define the dose distribution to aim for interior/superficial target volumes. A high dose is delivered over a small amount of fractions and a large offset of the source position can have an impact on dose delivery. It is recommended to verify the position of the source before treatment. The Varian BRAVOS afterloader has an automated position verification device called BRAVOS CamScale device (BCSD) available to verify the position of the source. Over one year conventional position verifications with a ruler have been performed in parallel to the BCSD approach and compared.

Materials and Methods

The BCSD is used to position the tip of the source or dummy cable (DC) at one of three predefined positions (90.0cm/120.0cm/150.0cm). Three cameras in the device are detecting the end position of the tip on a calibrated ruler with 0.05cm accuracy. Conventional position verification devices for the BRAVOS are not available anymore. Nevertheless, on a transparent transfer tube, a landmark at 90.0cm was tagged and the predefined source position visually via CCTV cameras checked. Close to the landmark, a ruler with a 1mm scale was placed. If the tip of the source was within ≤1mm the daily spot check passed.

Results

The median offset determined by the BCSD of the source and DC was 0.1mm with a maximum standard deviation of 0.4mm/0.2mm for the source/DC. The BRAVOS corrects the source position based on the actual DC position before treatment. Two times the DC position exceeded our threshold of 0.8mm during the daily check followed by a calibration of the source position. Hence, a maximum deviation of the source position was determined to 0.6mm. The conventional approach passed the visual check always with an accuracy of ≤1mm.

Conclusion

The BCSD was compared to a conventional approach for one year with reliable results and even higher accuracy.

Comparing dry-run and delivery modes for dynamic trajectory radiotherapy

Author: Paul-Henry Mackeprang[1]

Co-authors: Jenny Bertholet[1], Hannes A. Loebner[1], Claas Wessels[1,2], Silvan Mueller[1], Gian Guyer[1], Werner Volken[1], Michael K. Fix[1], Peter Manser[1]

[1]*Division of Medical Radiation Physics and Department of Radiation Oncology, Inselspital, Bern University Hospital, and University of Bern, Bern, Switzerland*

[2]*Varian Medical Systems Imaging Laboratory GmbH, Baden, Switzerland*

Purpose

Dynamic trajectory radiotherapy (DTRT) extends VMAT with dynamic table and collimator rotations during beam-on. Dry-runs are needed for safety purposes, as for example to check treatment plans for potential collisions. This study investigates if DTRT dry-runs accurately simulate the machine motion of DTRT via log-file analysis.

Materials and Methods

Eight DTRT treatment plans for clinically motivated head-and-neck cases were created for a TrueBeam system. Trajectory data were recorded every 20 ms during dry-runs and deliveries (with beam-on) and log files were retrieved after each run. Collimator rotation speed was used as a surrogate for application speed as it is rarely restricted by its maximum rotation speed but modulated down to wait for slower dynamic axes. Deviations between expected and actual values for gantry, table and collimator angles were determined.

Results

Three measurement sessions were available for analysis with 56 dry runs and 23 deliveries of 20 different trajectories. Dry-runs were faster, as indicated by a larger median absolute collimator rotation speed of 2.27°/s compared to 1.51°/s for deliveries. Overall, deviations of the analyzed axes were within clinical and interlock tolerance. Maximum gantry-angle deviations were larger in dry-runs (root-mean-square (RMS) 0.06°, max. 0.59°) than in deliveries (RMS 0.06°, max 0.33°). The same was found for table-angle deviations in dry-runs (RMS 0.11°, max. 0.26°) vs. deliveries (RMS 0.10°, max. 0.22°) and collimator-angle deviations in dry-runs (RMS 0.04°, max 0.43°) vs. deliveries (RMS 0.03°, max. 0.17°). A high correlation was found between speed and deviations of the table-angle (Spearman correlation coefficient 0.85 for dry-runs and -0.96 for deliveries, $p<0.05$).

Conclusion

The analyzed machine uncertainties are highly correlated to speed. Due to higher speed, deviations are larger in dry-runs than in deliveries, but overall small and still within interlock tolerance, indicating that dry-runs can be used for mechanical simulations of DTRT deliveries.

Development of a collision prediction tool using Blender for non-coplanar radiotherapy on a C-arm linear accelerator

Author: Gian Guyer[1]

Co-authors: Yanick Wyss[2], Silvan Mueller[1], Marco F. M. Stampanoni[3], Peter Manser[1], Michael K. Fix[1]

[1]*Division of Medical Radiation Physics and Department of Radiation Oncology, Inselspital, Bern University Hospital, and University of Bern, Bern, Switzerland*

[2]*ETH Zürich, Zürich, Switzerland*

[3]*Institute for Biomedical Engineering, ETH Zürich and PSI, Villigen, Switzerland*

Purpose

Non-coplanar treatment techniques on a C-arm linear accelerator have the potential to improve treatment plan quality in comparison to conventional coplanar volumetric modulated arc therapy (VMAT). During treatment planning of dynamic trajectory radiotherapy (DTRT), which extends VMAT by dynamic couch rotation, it is essential to know the gantry and table angle combinations leading to a collision during delivery. In this work, we developed a collision-prediction tool predicting gantry-table combinations leading to a collision of the gantry with the table or the patient.

Materials and Methods

A virtual linear accelerator model was created using Blender, a free and open- source 3D computer graphics software toolset, that can be accessed via an integrated python application programming interface. The virtual model includes the gantry, the table, the laser guard and a library of male and female patient models with different sizes and arm positions. The tool predicts for all gantry-table combinations discretized with a certain resolution whether there is a collision between gantry, table and patient model including a safety margin. For this purpose, the user has to specify the input of longitudinal, vertical and lateral table position, patient model from the library and safety margin. The collision prediction tool was experimentally verified. First, the tool is executed to generate collision predictions for each gantry-table combination with a 2° resolution for one input specification and second, these predictions are verified manually at a TrueBeam system.

Results

The true positive ratio, which is the ratio between the number of correctly predicted collision gantry-table combinations and the number of all predicted collision gantry-table combinations, is 82.4%. The true negative ratio, which is the ratio between the number of correctly predicted collision-free combinations and the number of all predicted collision-free combinations, is 99.9%.

Conclusion

A collision prediction tool for non-coplanar radiotherapy treatment planning was successfully developed. The tool enables non-coplanar plan creation with high safety for collision-avoidance.

Acknowledgements

This work was partially supported by grant 200021_185366 of the Swiss National Science Foundation and by Varian Medical Systems.

CyberKnife preliminary commissioning model for a twinned beam

Author: Valery Taranenko[1]

Co-authors: Matt Noll[1]

[1]*Accuray*

Purpose

To establish a beam twinning procedure and develop a model for accelerated TPS commissioning for all three collimators of CyberKnife M6 & S7 models.

Materials and Methods

Beam twinning was performed in two phases: initially with PTW Octavius 1000 SRS 2D panel with real-time feedback, then in 3D water tank with PTW SemiFlex 3D 0.3 cc chamber for cone-60 (0-300 mm PDD, 50 mm profiles) and the primary beam (50 mm profiles). Gamma matching against the twinning reference comprised: PDD 1mm/1% local, profiles 1mm/0.7% global. 10 linacs were twinned, then fully commissioned using PTW microDiamond with independent sets of fixed, Iris and MLC collimators. For each linac, all 35 beams (FS 5-115 mm) were measured for: TPR, dose profiles at 15, 100 and 300 mm depth, output factors (OF). The commissioning data were analyzed to develop a model for each of 35 beams with respect to OF, TPR, profiles. Each linac was tested against this BDI model using strict and relaxed matching criteria.

Results

Commissioning was greatly accelerated with PTW BeamScan tank and took 32 hrs/linac. Comparing each of 10 linacs vs the model, OF showed: FS 10+ mm 0.3%/0.5% (RMSE/max) errors, two smallest FS (5, 7.5 mm) > 0.5% errors. For TPR, gamma 1 mm/1% local in 0-200 mm, and 1.5% local in 200-300 mm passed 95+%. For profiles the following gamma passed 95+%: for cones & Iris, 0.3/0.6 mm (small/large FS), 0.5%, 0.7%, 1.5% global (15, 100, 300 mm depth); for MLC, 0.3-1 mm (smallest-to-largest FS), 1%, 1%, 1.5% global (same depths).

Conclusion

Preliminary model provides strict beam control deemed to be acceptable for SRS/SBRT. Two linac failures for energy twinning called for manufacturing improving. Iris radiation FS calibration, similar to MLC, can reduce its data variance.

Calculation of dosimetric parameters in paediatric phantoms using Monte Carlo techniques for 18F-FDG and the new TIAC

Author: Carlos V. G. Ferreira[1]

Co-authors: Bruno M. Mendes[2], Lucas Paixão[3], Thiago Lima[4], Telma C. F. Fonseca[5]

[1]*Universidade Federal de Minas Gerais*

[2]*CDTN*

[3]*Departamento de Anatomia e Imagem da Faculdade de Medicina da UFMG*

[4]*Luzerner Kantonsspital, Luzern, Switzerland*

[5]*Departamento de Engenharia Nuclear da UFMG*

Purpose

In nuclear medicine, one of the most used radiopharmaceutical is 18F-FDG, administered in paediatric and adult patients considering the same time-integrated activity coefficient (TIAC). Although, the IAEA recommends specific paediatric dosimetry. The objective of this work was to estimate the absorbed dose per injected activity and effective dose per injected activity for the 18F-FDG using two paediatric voxel phantoms (Baby and Child) using Monte Carlo techniques.

Materials and Methods

The radiopharmaceutical biokinetic data was obtained from the ICRP publication 128. Furthermore, the new TIAC values from a more recent publication were studied for the following organs: brain, urinary bladder wall, liver, heart wall, and lungs. The absorbed dose per injected activity (AD/IA) and effective dose per injected activity (E) values were calculated from the EGSnrc and MCNP6.1 for both phantoms and compared to the simulated data of pediatric voxel phantoms from the ICRP 128, MIRDcalc software, and available literature.

Results

Regarding AD/IA in organs, differences up to 61% and 115% were found for the Baby and 120% and 167% for the Child phantoms, respectively with 18F-FDG. For the FDG using the new TIAC a maximum difference of 244% was found. For E the maximum differences were 27% and 31% respectively for Baby and Child phantom for FDG administered.

Conclusion

New specific pediatric dosimetric data has been computed by this study using reference phantoms for Baby and Child and newly recommended TIAC. The calculated data represent a contribution to the AD/IA gap in knowledge.

Assessing the robustness of normal tissue complication probability of head and neck treatment plans to contouring uncertainties

Author: Lisa S. Fankhauser[1,2]

Co-authors: Hannes A. Loebner[1], Werner Volken[1], Marco F. M. Stampanoni[2], Daniel M. Aebersold[1], Peter Manser[1], Michael K. Fix[1], Paul-Henry Mackeprang[1]

[1]*Division of Medical Radiation Physics and Department of Radiation Oncology, Inselspital, Bern University Hospital, and University of Bern, Bern, Switzerland*

[2]*Institute for Biomedical Engineering, ETH Zürich and PSI, Villigen, Switzerland*

Purpose

To assess the robustness of normal-tissue complication probability (NTCP) scores for xerostomia and dysphagia in treatment plans for head and neck squamous cell carcinoma (HNSCC) using volumetric modulated arc therapy (VMAT) and dynamic trajectory radiotherapy (DTRT) to contouring uncertainties.

Materials and Methods

In order to assess robustness of NTCP scores, an in-house developed software framework for flexible robustness assessment is extended to uniformly enlarge, shrink or shift contours of organs at risks (OARs). It is then connected to NTCP calculation using xerostomia and dysphagia models used in the Dutch indication protocol for proton therapy for HNSCC (LIPPv2.2, grade ≥ II and ≥ III, respectively). The software is applied to VMAT and DTRT treatment plans for two example loco-regionally advanced HNSCC cases with bilateral elective nodal irradiation (all sequential boost to 60/66/70 Gy in 2 Gy per fraction). Robustness to systematic shrinking / enlarging of ±2 mm per contour and shifts of ±2 mm in all three directions of the OARs contained in the NTCP model is evaluated.

Results

Nominal (contours without shifts or size changes) DTRT plans for the two example cases score lower values compared to the respective VMAT plans for all investigated NTCP endpoints with up to -7.1% for xerostomia grade ≥ II for the first case. Deviations in NTCP scores were similar between cases (range 1.5% to 1.6% and 1.6% to 1.8%, respectively) and technique (range 1.6% to 1.8% for DTRT vs. 1.6% to 1.7% for VMAT). Larger deviations were observed for contour shifts (range 1.6% to 1.8%) compared to deviations resulting from size uncertainties (range 0.9% to 1.1%).

Conclusion

Software to assess NTCP robustness for HN cases to contouring uncertainties was successfully developed and applied to two cases. NTCP scores of both example HNSCC cases are less sensitive to systematic OAR contour shrinking / enlarging than shifts for the investigated uncertainties.

Disclosures

This work was partially supported by Varian Medical Systems and .

Clinical implementation of machine learning autoplanning for breast treatments: the CHUV recipe

Author: Michele Zeverino[1]

[1]*CHUV – Centre Hospitalier Universitaire Vaudois, Lausanne, Switzerland*

Purpose

To report a general framework for the clinical implementation of a machine learning (ML) autoplanning model in RayStation (RS) TPS.

Materials and Methods

ML autoplanning was developed for left-sided breast patients under deep-inspiration breath-hold treated with a double-arc VMAT technique. Different ML models (M) were built for two SIB prescriptions, 60/50Gy (M1) and 48/42.4Gy (M2), respectively. There were 4 sequential phases for each model: preparatory, learning, tuning, and commissioning. The preparatory phase aimed to improve the existing dose distributions used as model input for learning while providing a revised list of clinical goals for PTVs and OARs. Model learning was executed by RS. Model tuning was carried out on 5 patients previously treated to improve the automated dose distribution with respect to the clinical one. Commissioning was finally performed on 15 patients comparing automated vs clinical delivered plans.

Results

In the preparatory phase, 87% of plans were redesigned due to missing dose objectives or structures in the existing plan. This lead to improve clinical goals for all OARs ($p<0.05$ for right lung and heart maximum dose) while keeping the same level of target coverage and homogeneity. Model learning required 80 plans for both M1 and M2. M1 was developed first. Tuning for M1 required 4 models by RS before commissioning, while for M2 the second model was directly considered acceptable for commissioning. From the commissioning, autoplans resulted in general better or at least equivalent to clinical plans for both models. Differences statistically significant were observed for target coverage, left lung mean dose and right breast maximum dose for M1 and left lung for M2. The whole process took 6 and 4 months for M1 and M2, respectively.

Conclusion

Clinical implementation of left breast autoplanning in RS was effective. Revision of input data used for model learning and ML model improvement in the tuning phase have to be carried out carefully to avoid suboptimal model outputs.

Development of a lexicographic automatic intensity optimization process

Author: Hannes A. Loebner[1]

Co-authors: Paul-Henry Mackeprang[1], Jenny Bertholet[1], Silvan Mueller[1], Nathan Torelli[1], Gian Guyer[1], Marco F. M. Stampanoni[2], Michael K. Fix[1], Peter Manser[1]

[1]*Division of Medical Radiation Physics and Department of Radiation Oncology, Inselspital, Bern University Hospital, and University of Bern, Bern, Switzerland*

[2]*Institute for Biomedical Engineering, ETH Zürich and PSI, Villigen, Switzerland*

Purpose

To develop an automatic intensity optimization (AIO) process for volumetric modulated arc therapy (VMAT) and intensity-modulated radiotherapy (IMRT), using the Eclipse scripting API (ESAPI).

Materials and Methods

A multi-round and multi-group lexicographic optimization process is developed interfacing the Eclipse treatment planning system via ESAPI. The input of the AIO process is the field setup for the patient and a treatment site-specific starting list of objectives consisting of dose-volume and mean dose objectives for target volumes and organs-at-risk (OARs), ranked in priority groups (PG) according to their clinical importance. The PGs are optimized in multiple sequential optimizations using the Eclipse Photon-Optimizer (PO). After each PO optimization, results are pinned by additional objectives with higher optimization weight at the achieved objective results. In subsequent PO optimizations over PGs, objectives are hardened towards favourable dose, if the previous objective results of other PGs are not deteriorated by the hardened objective. The lexicographic ordering of the AIO process is verified using a synthetic water cylinder with central cylindrical target and three concentric symmetrically distributed OARs, with the same objectives for each OAR assigned to different PGs. Additionally, pareto-optimality is checked by manual re-optimization. The AIO is further applied to a clinically motivated head-and-neck cancer case. For both cases, treatment plans with two full VMAT arcs are generated.

Results

For the synthetic case, OARs show mean dose differences of >10%, with higher dose in OARs ranked in lower PGs, confirming lexicographic ordering. Manual hardening of one objective leads to worse results for other objectives, confirming pareto-optimality. For the clinically motivated plan, AIO spared OARs from higher-ranked PGs better than manual optimization (spinal cord Dmax 13.4 Gy vs. 19.4 Gy), with higher doses in OARs from lower-ranked PGs (right submandibular gland Dmean 15.3 Gy vs. 11.2 Gy).

Conclusion

Successful implementation of a lexicographic AIO process for VMAT and IMRT plans using ESAPI is demonstrated on an academic and a clinically motivated case.

Disclosures

This work was partially supported by Varian Medical Systems and by grant 20021_185366 of the Swiss National Science Foundation.

Session II: Radiobiology, Radiomics, Adaptive RT

27.10.2022, 13:45 – 15:15

Chair: Dr. Jenny Bertholet,

Inselspital – University Hospital Bern

Dose guidance in daily adaptive proton therapy: Predicting the cumulative treatment dose

Author: Evangelia Choulilitsa[1]

Co-authors: Damian C. Weber[2,3,4], John A. Lomax[1], Francesca Albertini[1]

[1]*PSI – Paul Scherrer Institute, Villigen, Switzerland*

[2]*Center for Proton Therapy, Paul Scherrer Institute, Villigen, Switzerland*

[3]*Department of Radiation Oncology, University Hospital Zurich, Zurich, Switzerland*

[4]*Department of Radiation Oncology, University Hospital Bern, Bern, Switzerland*

Purpose

The prescribed treatment dose, routinely calculated on the planning CT and approved by the radio-oncologist, is assumed as the dose applied for the whole treatment (ApprovedTD). However, in online daily adaptive proton therapy (DAPT), the plan is optimized on the daily CT to correct for anatomical daily changes, while the patient is lying on the treatment table. Intrinsically, both the daily delivered dose and the total delivered treatment dose (DeliveredTD) can be more accurately estimated via dose accumulation. Before the end of the treatment series however, and to facilitate fraction-specific adjustments and day-to-day decisions, it can be advantageous to predict the DeliveredTD at the end of therapy dose as the treatment is progressing. In this study, two different approaches for predicting the total delivered treatment dose (PredictedTD) as part of a DAPT workflow are being presented.

Materials and Methods

For both models and every fraction, each daily adapted plan is accumulated on the planning CT for the already delivered fractions. The doses for the prospective fractions are then filled in in two ways. With either the initial reference plan optimised on the planning CT multiplied by the remaining fractions, or with the last daily delivered plan multiplied by the remaining fractions. Consecutively, the resulting PredictedTP is calculated for every fraction and compared with both the DeliveredTD and the ApprovedTP. All the aforementioned calculations are performed for 2 cases with 18 daily CTs each in our house-developed treatment planning system.

Results

For both cases, differences between the PredictedTP and the DeliveredTP are smaller than 0.5GyRBE for more than 87% and of 93% of organ-at-risk and target voxels respectively.

Conclusion

Early findings suggest that with both models it is indeed possible to accurately predict the delivered treatment dose. This creates new possibilities during DAPT to make informed daily decisions based on the delivered cumulative treatment dose.

Dosimetric accuracy verification of treatment plans generated during online adaptive radiotherapy

Author: Daniel Schmidhalter[1]

Co-authors: Dominik Henzen[1], Hossein Hemmatazad[1], Mohamed Sheland[1], Daniel M. Aebersold[1], Michael K. Fix[1], Peter Manser[1]

[1]*Division of Medical Radiation Physics and Department of Radiation Oncology, Inselspital, Bern University Hospital, and University of Bern, Bern, Switzerland*

Purpose

When performing online adaptive radiation therapy (ART), dosimetric measurements of the treatment plan of the day with the aid of a phantom before applying the dose to the patient is not possible. Typically, a dose recalculation with an independent system is done in this situation. In order to verify the accuracy of the dose distributions delivered by these online ART plans, for a series of indications and treatment techniques phantom measurements were performed retrospectively.

Materials and Methods

35 plans (10 Esophagus, 10 Lower esophagus, 10 Prostate, 5 Rectum with in total 20 IMRT and 15 VMAT plans) of 7 different patients generated during online adaptive sessions on the Ethos system were calculated and applied to the cylindrical Delta4 phantom. The measured and calculated dose distributions were compared with the gamma method using the following criteria: 3% dose difference (global), 3 mm distance to agreement, 20% dose threshold.

Results

The mean gamma passing rate over all cases was 98%. The lowest passing rate was 95.8% and was found for an IMRT plan treated in the Esophagus region. Mean passing rates for the different indications and techniques were found as follows: 96.1%, 100% for Esophagus (IMRT, VMAT), 99.9%, 100% for Lower esophagus (IMRT, VMAT), 100%, 99.9% for Prostate (IMRT, VMAT) and 100% for Rectum (IMRT).

Conclusion

For the new treatment modality, online ART at the Ethos system, we demonstrated the accuracy of the dose distributions delivered by plans generated during the online ART session, with the aid of phantom measurements for different indications and two different treatment techniques (IMRT and VMAT).

MET-targeting CAR T cells enhance tumor cell killing and cytokines release in glioma models when combined with radiation therapy

Author: Lusine Hovhannisyan[1,2]

Co-authors: Daniel M. Aebersold[2], John Maher[4], Adrian F. Ochsenbein[2,3], Carsten Riether[2,3], Michaela Medová[1,2], Yitzhak Zimmer[1,2]

[1]*Department of Radiation Oncology, Inselspital, Bern, Switzerland*

[2]*Department for BioMedical Research, University of Bern, Bern, Switzerland*

[3]*Department of Medical Oncology, Inselspital, Bern, Switzerland*

[4]*Faculty of Life Sciences & Medicine, King's College London, UK*

Purpose

Glioblastoma (GBM) is the most frequent primary brain tumor with dismal prognosis after radiation therapy, a standard treatment option for this disease. Recently, RT has been investigated as a mediator of effects of T cell-based therapies in the context of immunosuppressive GBM microenvironment. The MET receptor is an oncogene involved in radiation resistance, and stem-like properties of GBM. We study the impact of MET-targeting chimeric antigen receptor (CAR) T cells (MET-CAR T cells) combined with radiation in GBM, and hypothesize that this combination acts synergistically in terms of tumor growth control.

Materials and Methods

We co-cultured MET-CAR T cells with adherent (2D) and stem-like (3D) human GBM cells with or without RT and assessed the killing efficiency and cytokine production of CAR T cells.

Results

Our results indicate that 5Gy radiation combined with MET-CAR T cells increases their potential in tumor cell killing. We observed increased CAR T cells effect at lower CAR T to target cells ratios when combined with radiation, even when radiation treatment alone did not lead to a significant decrease in GBM cell viability. This phenomenon was similar in both types of cell lines as well as across different levels of MET expression, and different sensitivity to CAR T cells. The mechanisms behind this observation were investigated via intracellular cytokine measurements. The most prominent response was in TNF-alpha expression. Increase in Granzyme B expression was observed in co-culture with some of the GBM cell lines and was more prominent in CD8+ subpopulation of CAR T cells. Increase in IFN-gamma was observed in some adherent glioma cell lines but was absent in co-culture with stem-like glioma cell lines. Our pilot in vivo study in orthotopic GBM model demonstrated tumor reduction after 48h of intravenous and intracranial injection of MET-CAR T cells. The RT-CAR T combination studies are to follow.

Conclusion

In conclusion, our data demonstrates the potency of MET-CAR T cells against GBM, and increased efficiency when combined with radiation. The suggested mechanism is the increased activation of T cells in TNF-alpha-dependent-manner.

Fractionated radiation therapy increases Siglec-7 and -9 ligands expression in cancer cells

Author: Marjolaine Hugonnet[1]

Co-authors: Lusine Hovhannisyan[2,3], Michaela Medová[2,3], Yitzhak Zimmer[2,3], Stephan von Gunten[1]

[1]*Institute of Pharmacology, University of Bern, Bern, Switzerland.*

[2]*Radiation Oncology, Department for BioMedical Research, University of Bern, Bern, Switzerland.*

[3]*Radiation Oncology Clinic, University Hospital Bern, Bern, Switzerland.*

Purpose

Radiation therapy is a standard therapy option in many cancer types. Recently, improved effects were observed when radiation therapy was combined with immunotherapy such as immune checkpoint inhibitors. Indeed, radiation therapy has a systemic immunomodulatory effect by stimulating cancer immunity cycle through the release of cancer antigens and improving immune infiltration. Besides, radiation can also inhibit immune response by an increase in expression of immune suppressor ligands including PD-L1. Siglec ligands are molecules expressed on cancer cells that inhibit immune response by binding to the receptors on immune cells. The purpose of this project is to study the role of Siglec ligands in the context of radiation therapy and immune response.

Materials and Methods

We used a panel of human and mouse cancer cell lines (LN18, LN229, SKOV-3, K562, P815) to study Siglec ligands expression after single dose (2, 5, 10 Gy) and fractionated (5x2Gy) radiation. Cells were irradiated and Siglec ligands expression was measured via flow cytometry. Mean fluorescence intensity was quantified. To assess the impact of irradiation on immune response, cells were irradiated and tested in co-culture with NK and CAR T cells. Cells lacking Siglec ligands due to neuraminidase treatment or Cytidine Monophosphate N-Acetylneuraminic Acid Synthetase (CMAS) knockout (KO) were used as negative controls.

Results

Our results indicate an increase of Siglec-7 and -9 ligands expression in the studied cancer cell lines upon radiation therapy, especially after fractionated regimen. Due to this increase in Siglec ligands, fractionated radiation therapy of LN18 and K562 decreased NK cell-mediated anti-tumor responses, whereas neuraminidase treatment of cancer cells improved NK-cell killing. In addition, CAR T-mediated killing was more effective in CMAS KO cells and radiation sensitivity was increased in CMAS KO cell lines.

Conclusion

This study is the first to show that radiation can activate immune suppressor Siglec ligands expression on the surface of cancer cells. This effect may impair concurrent immune activation, hence should be addressed by combining radiation with therapeutics that block Siglec-Siglec ligands axis.

Influence of image resolution and extraction software on the stability of radiomic features

Authors: Lars Widmer[1], Hubert Gabrys[1]

Co-authors: Simon Burgmeister[1], Lucas Basler[1], Marta Bogowicz[1], Reinhard Dummer[1], Robert Förster[1], Matthias Guckenberger[1], Sabrina Hogan[1], Martin Huellner[1], Mitch Levesque[1], Matea Pavic[1], Diem Vuong[1], Stephanie Tanadini-Lang[1]

[1]*Department of Radiation Oncology, University Hospital Zurich, Zurich, Switzerland*

Purpose

Before the extraction of radiomic features, images are usually interpolated to a common resolution. Furthermore, a number of different radiomic feature extraction software exist. Here, we investiage how choice of interpolation resolution and feature extraction software affects stability of radiomic features.

Materials and Methods

Following work quantifies this influence on the radiomic features by comparing pre-treatment CT and PET images of melanoma patients resized to 1 mm and 2 mm resolution and the two IBSI-compliant feature extraction platforms Z-Rad and PyRadiomics. The stability is assessed with the ICC(3,1) (intraclass correlation coefficient) according to the Shrout and Fleiss convention. The total set of 1413 (856) radiomic features extracted, included 25 (16) shape, 19 (21) intensity, 137 (75) texture and 1232 (744) wavelet features for Z-Rad (PyRadiomics). To compare PyRadiomics and Z-Rad, a set of 686 (470) features, consisting of 9 (9) shape, 17 (17) intensity, 60 (36) texture and 600 (408) wavelet features was defined for CT (PET) images.

Results

Both feature extraction platforms provide high stability ($\overline{ICC}$> 0.95, *first quartile*> 0.9) for shape and intensity features in both imaging modalities when comparing 1 mm with 2 mm scaling resolution. However, there are a few outliers with low intraclass correlation present. Texture features show good stability ($\overline{ICC}$> 0.8, *first quartile*> 0.5) while most wavelet features show poor intraclass correlation. Only the LLL wavelet features show good stability ($\overline{ICC}$> 0.8, *first quartile*> 0.55). Comparing Z-Rad and PyRadiomics led to a high intraclass correlation for intensity and texture features with both resolutions ($\overline{ICC}$> 0.95, *first quartile*> 0.85) in CT images. Shape features showed good stability ($\overline{ICC}$= 0.91, *first quartile*= 0.62) while wavelet features overall showed a low ICC ($\overline{ICC}$= 0.42, *first quartile*= 0.20). The analysis with PET images showed worse intraclass correlation for all general types.

Conclusion

An overall good stability of shape, intensity and texture features has been shown in the comparisons of two different image resolutions and two different feature extraction platforms. However, there are several outliers in each of these general types, explainable by extraction parameters, image properties and feature definition.

Magnetic resonance imaging radiomic features stability in brain metastases

Author: Zahra Khodabakhshi[1]

Co-authors: Hubert Gabrys[2], Philipp Wallimann[2], Matthias Guckenberger[2], Nicolaus Andratschke[2], Stephanie Tanadini-Lang[2]

[1]*University of Zurich, Zurich, Switzerland*

[2]*Department of Radiation Oncology, University Hospital Zurich, Zurich, Switzerland*

Purpose

In radiomic studies, robustness of models can be challenging due to variations in feature values caused by different scanners and imaging protocols. This problem is most prominent in magnetic resonance imaging (MRI) due its high sensitivity to imaging parameters. This study aims to assess the impact of image preprocessing, and image-normalization on the stability of MRI-based radiomic features. We also report a radiomics model to classify primary cancer site based on radiomic characteristics of metastases.

Materials and Methods

Twenty-five patients with brain metastases and two MRI scans at different time points were enrolled in this study. The images were discretized using fixed bin number (FBN) (16, 32, 64,128, and 256) or fixed bin size (FBS) (average volume of interest (VOIs) intensity/bin numbers). Four MRI intensity normalization techniques, including Nyul, Z-score, White Stripe, and an in-house developed method called N-Peaks, were applied to the images. Radiomics feature extraction was performed using Pyradiomics. Intra class correlation coefficients (ICC) were calculated for all analyzed preprocessing methods. Features with ICC>0.8 were considered stable. For the classification task, 64 brain metastases patients with primary lung (n=33) or melanoma (n=31) cancer were included and radiomic model performance for different preprocessing methods was evaluated.

Results

The percentage of stable features increased with increasing bin number or decreasing bin sizes for all configurations. For the five normalization variants (non-normalized, Nyul, N-peaks, White Stripe and Z-Score), we found the following percentages of stable features. Using FBN = 64: 21%, 20%, 21%, 19%, and 19% respectively. Using FBS = (average VOIs intensities/64): 7%, 13%, 11%, 10%, and 12%. For the classification task, the model based on Nyul normalization and FBN gray level discretization had the highest AUC of 0.69 ±0.11.

Conclusion

The effect of normalization on the stability of radiomic features highly depends on preprocessing methods. Using FBN resulted in a higher percentage of stable features and no clear benefit from intensity normalization. For FBS, the stability of features is improved after intensity normalization. FBN resulted in better classification performance.

PET/CT radiomics for prediction of hyperprogression in metastatic melanoma patients treated with immune checkpoint inhibitors

Author: Hubert Gabrys[1]

Co-authors: Diem Vuong[1], Maiwand Ahmadsei[1], Lucas Basler[1], Marta Bogowicz[1], Simon Burgermeister[1], Reinhard Dummer[1], Robert Förster[1], Matthias Guckenberger[1], Sabrina Hogan[1], Martin Huellner[1], Ken Kudura[1], Mitch Levesque[1], Matea Pavic[1], Stephanie Tanadini-Lang[1]

[1]*Department of Radiation Oncology, University Hospital Zurich, Zurich, Switzerland*

Purpose

This study evaluated pretreatment FDG-PET/CT-based radiomic signatures for prediction of hyperprogression in metastatic melanoma patients treated with immune checkpoint inhibition (ICI).

Material and methods

56 consecutive metastatic melanoma patients treated with ICI and available imaging were included in our study and 330 metastatic lesions were individually segmented on pre-treatment CT and 2[18F]fluoro-2-deoxy-D-glucose (FDG)-PET imaging. Lesion hyperprogression (HPL) was defined as lesion progression according to RECIST 1.1 and doubling of tumor growth rate, whereas patient hyperprogression (PD-HPD) was defined as progressive disease (PD) according to RECIST 1.1 and presence of at least one HPL. Pre-treatment PET/CT-based radiomic signatures were used to build models predicting HPL at three months after start of treatment. The models were internally validated with nested cross-validation.

Results

Of all lesions, 69 (20.9%) were identified as progressing at 3 months. 29 of these lesions were classified as hyperprogressive, thereby showing a HPL rate of 8.8%. PD-HPD patients constituted 57.1% of all PD patients. PD-HPD was negatively related to patient overall survival with HR=8.52 (95%CI 3.47-20.94). Our best model predicting HPL at three months after the start of treatment achieved AUC=0.753 +/- 0.028 in training and AUC=0.685 +/- 0.089 in testing. The model relied on CT-based histogram and texture features.

Conclusion

FDG-PET/CT-based radiomic signatures yield potential for pretreatment prediction of hyperprogression, which may contribute to reducing the risk of delayed treatment adaptation in metastatic melanoma patients treated with ICI.

Feasibility and mechanical accuracy of gated dynamic trajectory radiotherapy

Author: Hannes A. Loebner[1]

Co-authors: Daniel Frauchiger[1], Dario Terribilini[1], Silvan Mueller[1], Gian Guyer[1], Paul-Henry Mackeprang[1], Marco F. M. Stampanoni[2], Michael K. Fix[1], Peter Manser[1], Jenny Bertholet[1]

[1]*Division of Medical Radiation Physics and Department of Radiation Oncology, Inselspital, Bern University Hospital, and University of Bern, Bern, Switzerland*

[2]*Institute for Biomedical Engineering, ETH Zürich and PSI, Villigen, Switzerland*

Purpose

To experimentally assess the technical feasibility and quantify the mechanical accuracy of respiratory gating during dynamic trajectory radiotherapy (DTRT) plan delivery. DTRT extends VMAT by dynamic table and collimator rotation during beam-on.

Materials and Methods

An HexaMotion motion stage positioned on the treatment table of a TrueBeam system is used to reproduce four different breathing motion traces recorded in patients typical, high frequency, predominantly left-right and baseline shift, each with combined motion in superior-inferior, anterior-posterior, and left-right directions. A DTRT plan for a clinically motivated lung case is delivered both with and without gating on a TrueBeam system in Developer Mode. For gating, the real-time positioning management system is used to trigger amplitude gating based on the main motion axis (either superior-inferior or anterior-posterior) with gating window between 4 and 6 mm depending on the motion trace. Mechanical accuracy is assessed from TrueBeam trajectory log files as the deviation between actual and expected machine positions of gantry, table and collimator angle and positions of moving MLC leaves.

Results

DTRT delivery was successfully gated with the gantry, table and collimator rotating back during beam-hold and resuming motion at beam-on (i.e., when entering the gating window). The mean root-mean-square deviation between expected and actual position for DTRT delivery with (resp. without) gating were 0.04° (0.03°) for gantry angle, 0.05° (0.09°) for table angle, 0.02° (0.03°) for collimator angle and 0.002 mm (0.002 mm) for moving leaves' positions. Maximum deviations were 0.13° (0.10°) for gantry angle, 0.14° (0.15°) for table angle, 0.08° (0.08°) for collimator angle and 0.003 mm (0.004 mm) for moving leaves positions.

Conclusion

A gated DTRT plan was successfully delivered on a TrueBeam system with machine accuracy in gantry table and collimator angle and MLC leaf positions similar to un-gated delivery.

Disclosures

This work was partially supported by Varian Medical Systems.

Influence of two-level quality assurance methodology on safety margins size and planning target volumes in frameless mask-based image-guided stereotactic intracranial radiosurgery and radiotherapy

Author: Sergejs Popovs[1]

Co-authors: Käthy Haller[1], Fabrizio Storelli[1], Uwe Schneider[1]

[1]*Institute for Radiotherapy, Radiotherapy Hirslanden AG, Zürich, Switzerland*

Purpose

To estimate influence of adding tolerance levels (TL) to ultimate action levels (AL) in quality control (QC) of equipment geometrical precision in stereotactic radiotherapy on size of safety margins (SMs) and, consequentially, planning target volumes (PTVs) in frameless image-guided stereotactic intracranial radiosurgery and radiotherapy (SRS/SRT) delivered with the Accuray CyberKnife 6D skull tracking and fixed aperture conical collimators (6DST).

Materials and Methods

AL and TL for SRS/SRT QC are employed in our institution. If errors fall between TL and AL one can operate till end of the day and then adjust. AL are set according to SSRMP recommendations No.18 tolerance levels (R.18.TL). Additionally, tighter TL are used, based on institution data and other recommendations. For End-to-End phantom-tests (E2E) AL is 1.00 mm 3D radial error and TL is 0.75 mm deviation in any direction. SMs were estimated using van Herk's recipe. Institution (E2E, intrafraction, σp) and literature (MRI-CT registration, GTV delineation) data was used. Prescription isodoses range was 70-80%. E2E errors distribution for R.18.TL was estimated by corresponding expansion of institution data.

Results

Mean E2E errors ±1 SD (RMS) were 0.13±0.26 (0.28), 0.19±0.17 (0.25), -0.09±0.14 (0.16) mm in Superior-Inferior (SI), Right-Left (RL), Anterior-Posterior (AP) directions, respectively. Combined SD of intrafraction errors was 0.07, 0.10 and 0.11 mm (SI, RL, AP). SD of GTV delineation/MRI-CT registration errors was 0.29, 0.28, 0.30 / 0.57, 0.33, 0.32 mm (SI, RL, AP). σp was 3.60 mm. AL-TL-based anisotropic 6DST SMs was 1.8, 1.3, 1.2 mm (SI, RL, AP). Allowing R.18.TL, results in SMs 2.2, 1.9,1.9 mm (SI, RL, AP). Implementation of two-level E2E tolerances resulted in reduction of PTV/GTV volume ratio by 24% for 1.0 cm, 14% for 2.0 cm and 8% for 4.0 cm diameter spherical GTV, respectively.

Conclusion

Establishing TL additional to AL in SRS/SRT QC allows substantial reduction of SMs. This translates in substantial decrease in PTV shell volumes, especially for smaller GTVs, which may be especially important for patients receiving biological therapy in addition to SRS/SRT.

Session III: Imaging

28.10.2022, 10:15 – 11:55

Chair: Dr. Lukas Wissmann,
Spital Thurgau

Towards more realistic 4DCT(MRI) numerical lung phantoms

Author: Alisha Duetschler[1], Timothy Jenny[1]

Co-authors: Sairos Safai[1], Damien C. Weber[1], Antony J. Lomax[1], Ye Zhang[1]

[1]*PSI – Paul Scherrer Institute, Villigen, Switzerland*

Purpose

Numerical 4D phantoms are a valuable tool for simulations and developments in 4D radiotherapy and image guidance. We present an upgrade of the 4DCT(MRI) lung phantoms, integrating realistic respiratory ribcage motion and further enhancing the lung density representation throughout the breathing cycle.

Materials and Methods

Synthetic 4DCTs, referred to as 4DCT(MRI)s, are based on density information of reference CTs combined with motion from multiple-breathing-cycle 4DMRIs. First, the motion of the lungs and ribcage was independently extracted from 4DMRIs using deformable image registration (DIR). After establishing inter-subject correspondence between the CT and MRI anatomy through the DIR of binary masks of the lungs and ribcage, the 4DMRI motion was applied to the corresponding locations in the CT. The resulting deformation vector fields (DVF) was further post-processed to preserve sliding organ motion along the chest wall. Lastly, lung densities were scaled according to the Jacobian determinant of the DVFs, which represents local lung volume changes. The new workflow was validated using four clinical 4DCTs and compared to the old workflow (without ribcage motion and density scaling). For this purpose, synthetic 4DCTs (referred to as 4DCT(CT)s), were generated using the motion from the 4DCTs themselves. 4DCT(CT)s were created using the old and new workflow and compared to the original 4DCTs in terms of mean lung density and through pencil beam scanned (PBS) proton 4D dose calculations.

Results

The newly implemented lung density scaling resulted in a reduction of the maximum difference in mean lung HU from 45 HU to 12 HU between the 4DCTs and the corresponding old and new 4DCT(CT)s, respectively. Comparison of 4D dose distributions of PBS plans calculated on the new 4DCT(CT)s and 4DCTs resulted in very high 2%/2mm gamma pass rates (>97%), which were on average 1.4% higher than for the old 4DCT(CT)s.

Conclusion

The 4DCT(MRI) workflow was successfully improved and the resulting 4DCT(MRI) lung phantoms demonstrate realistic respiratory ribcage motion with sliding organ motion along the chest wall and a more accurate representation of respiratory induced lung density changes.

New methodology to assess spatiotemporal image quality on fluoroscopy devices

Author: Damien Racine[1]

Co-authors: Anais Viry[1], Marie Nowak[1], Pascal Monnin[1]

[1]*CHUV – Centre Hospitalier Universitaire Vaudois, Lausanne, Switzerland*

Purpose

The planar formulation of the noise equivalent quanta (NEQ) and detective quantum efficiency (DQE) used to assess the image quality of projection images does not deal with the influence of temporal resolution on signal blurring and image noise. These metrics require correction factors based on temporal resolution when used for dynamic imaging systems such as fluoroscopy. Additionally, the standard NEQ and detector DQE are determined on pre-processed images in scatter-free conditions for effective energies produced by additional aluminium or copper filters that are not representative of clinical fluoroscopic procedures. In this work, we developed a method to measure 'frame NEQ' and 'frame system DQE' which include the temporal frequency bandwidth and consider the anti-scatter grid, the detector and the image processing procedures for beam qualities with scatter fractions representative of clinical use.

Materials and Methods

We used a solid water phantom to simulate a patient and a thin copper disc to measure the spatial resolution. The copper disc, set in uniform rectilinear motion in the image plane, assessed the temporal resolution. These new metrics were tested on two fluoroscopy systems, a C-arm and a floor-mounted cardiology, for multiple parameters: phantom thicknesses from 5 to 20 cm, frame rates from 3 to 30 fps, spatial and temporal image processing of different weights.

Results

The frame NEQ correctly described the image quality for different scatter conditions, temporal resolutions and image processing techniques. The frame system DQE varied between 0.38 and 0.65 within the different beam and scatter conditions, and correctly mitigated the influence of spatial and temporal image processing.

Conclusion

This study introduces and validates an unbiased formulation of in-plane NEQ and system DQE to assess the spatiotemporal image quality of fluoroscopy systems.

Fluoroscopy-guided intervention for a splenic artery aneurysm during pregnancy: Evaluation and optimization of fetal radiation exposure

Author: Hannah J. Eggimann[1]

Co-authors: Enrique A.-Lafont[2], Jörg Binder[1], Friedemann Herberth[3], Hans Schiefer[3], Gerd Lutters[1], Stephan Scheidegger[4]

[1]*Fachstelle Strahlenschutz & Medizinphysik, Kantonsspital Aarau, Aarau, Switzerland*

[2]*Interventionelle Radiologie, Kantonsspital St Gallen, St Gallen, Switzerland*

[3]*Klinik für Radio-Onkologie, Kantonsspital St Gallen, St Gallen Switzerland*

[4]*ZHAW School of Engineering, Winterthur, Switzerland*

Purpose

A splenic artery aneurysm during pregnancy poses a possibly life-threatening risk to the patient and is challenging to treat. One treatment option is fluoroscopy-guided embolization, which is however often met with apprehensiveness by the medical team due to potential prenatal radiation exposure. Therefore, knowledge of the expected uterus dose and effective radiation protection measures is critical for an informed decision on the course of the treatment. This work evaluates fetal radiation exposure during a clinical case of a splenic artery aneurysm successfully treated by fluoroscopy-guided coil embolization, i.e. simulation and validation thereof, and identifies key factors determining the uterus dose. The results inform best practice radiation protection measures and procedures for planning similar fluoroscopic interventions on pregnant patients.

Materials and Methods

The expected uterus dose from the clinical case is simulated with the Monte-Carlo-based software PCXMC and different scenarios are considered to identify key drivers of fetal radiation exposure for similar interventions. To validate the simulation results, TLD measurements within an Alderson phantom are performed.

Results

The fetal dose from the intervention was simulated to be below 0.5 mGy. At this dose level, no adverse deterministic effects or significant increase in the likelihood of childhood cancer are expected. However, the dose can increase significantly if the x-ray fields are uncollimated, the distance between the inferior field edge to the uterus is small, or if the uterus is in the primary beam during femoral access. Uncertainty in the uterus position during the intervention is a non-negligible source of error in the simulation. The simulation findings were confirmed by TLD measurements within the phantom.

Conclusion

The simulation and measurements demonstrate similar fluoroscopy-guided interventions on a pregnant patient are possible with minimal fetal exposure. Simulation of the x-ray fields allows reliable retrospective estimation of the dose to the unborn and to prospectively advise the medical team on radiation protection measures or whether techniques without ionizing radiation should be considered.

Clinical commissioning of the MARS spectral photon-counting CT and its first clinical application for the diagnosis of crystal arthropathies

Author: Lucia G. Manzano[1]

Co-authors: Pascal Monin[1], Yann Sayous[2], Damien Racine[1], Jérôme Damet[1], Fabio Becce[1], Anais Viry[1]

[1]*CHUV – Centre Hospitalier Universitaire Vaudois, Lausanne, Switzerland*

[2]*University of Canterbury, Christchurch, New Zealand*

Purpose

To assess the image quality and dose performance of the first SPCCT for extremity imaging, and to demonstrate its clinical benefit for the diagnosis and management of crystal arthropathies.

Materials and Methods

The MARS Extremity 5x120 is a small-bore point-of-care SPCCT scanner designed for conducting clinical investigations on the upper extremities. We carried out the first full clinical commissioning of the scanner, which included basic and adapted image quality and radiation dose metrics, dedicated phantoms, and automated analysis techniques. Basic metrics were evaluated to determine whether they met international standards for quality assurance and national regulations. Material discrimination capabilities were evaluated using various high- and low-Z materials. The volume dose index (CTDIvol) was measured on a custom-made 10-cm diameter CTDI phantom. In order to assess the potential of the MARS scanner in detecting, quantifying and distinguishing different crystals, we developed a custom phantom that mimics peripheral joints with synthetic crystal inserts at concentrations typically found in patients with crystal arthropathies.

Results

Image quality metrics, such as CT number of water, uniformity, noise level and slice thickness, satisfies all technical specifications and comply with international standards. The in-plane spatial resolution was 1.5 lp/mm (10% MTF), about 3 times higher compared to conventional CT. An excellent longitudinal spatial resolution of 5.0 lp/mm (10% MTF) was obtained. A good spectral correlation and linearity was found. The CTDIvol for the routine hand and wrist protocol was 9.81 mGy, equivalent to 3.82 mGy for a standard 32 cm CTDI phantom. Preliminary results from the discrimination potential for various crystals involved in crystal arthropathies are very promising.

Conclusion

SPCCT are emerging imaging modalities that promise to revolutionize clinical practice allowing new diagnostic features through the detection, identification and quantification of multiple materials simultaneously. Nonetheless, adapted image quality and radiation dose metrics are necessary to fully benefit from the spectral information. Results from this study show that the SPCCT have the potential to provide useful clinical information for enhanced diagnosis of crystal-related arthropathies.

Self-supervised skin lesion screening in dermatology consultation

Author: Javier B. Garcia[1]

Co-authors: Nicolaus Andratschke[1], Ralph P. Braun[1], Quentin Lohmeyer[2], Stephanie Tanadini-Lang[1], Vullnet Useini[2]

[1]*Department of Radiation Oncology, University Hospital Zurich, Zurich, Switzerland*

[2]*ETH Zürich, Zürich, Switzerland*

Purpose

Early detection is essential for optimal survival of patients diagnosed with melanoma. To counteract the bottleneck of shortage of specialists and to enable at-risk patients to receive a faster consultation, an AI decision support tool is proposed. This will enable more efficient consultation, patients' risk assessment, and overall better treatment outcomes for patients.

Materials and Methods

During skin lesion screening, the dermatologists identify suspicious lesions or "ugly duckling" (UD) by direct comparison with all lesions on the same patient. This can be modeled as an outlier detection problem. Our dataset is composed by 90 high-resolution total-body images (TBI) acquired using Fotofinder© devices. For single lesion detection, a YOLOR architecture is trained on labeled patients in a supervised manner to automatically detect and extract all the lesions. The extracted lesions are then clustered in a self-supervised manner using DINO architecture. These embeddings are then used to find the outliers and potential UDs. The UD score for embedded lesion of a patient is calculated using the normalized cosine distance value from the average of his embedded lesions. The detection algorithm was trained in 15 labeled patients and tested on the dorsal region of 4 unseen patient images. For each of the 4 patients, the ten highest scoring lesions are presented. For validation these are compared against the top 4 UD by a pigmented lesion expert.

Results

Lesion detector achieved an average recall of 91% and precision of 88% with an IoU threshold of 0.5. The outlier selection and a 2D-tsne-representation of the embedded lesions show promising results and agreed with visual validation by a pigmented lesion expert.

Conclusion

An end-to-end DL pipeline for automatic lesion detection and self-supervised identification of "ugly ducklings" has been implemented and successfully tested on 4 unseen patients. Further clinical validation against expert's prediction is foreseen as well as implementation in routine consultation workflow.

Comparison of mammography image quality across different radiology departments based on the IAEA technical report on the Implementation of an Automated Quality Control Programme

Author: Milena C. Gravinatti[1]

Co-authors: Justus Roos[1], Simone Schrading[1], Mirjam Heinrich[1], Thiago Lima[1]

[1]*Luzerner Kantonsspital, Luzern, Switzerland*

Purpose

Regular quality control (QC) testing of radiological images has been overlooked throughout the world, although it has been shown to reduce patient radiation exposure and improve image quality [1]. The aim of this project is to test the framework for QC of mammographic imaging systems proposed by IAEA Human Health Series n. 39 and to characterize the response from different mammography devices based on image quality and dose across different centres in the central Switzerland region.

Materials and Methods

The proposed phantom was manufactured in-house for the purpose of this work with the following specifications: A PMMA target plate made of a 24cm×30cm×0.5cm, with a copper test object of 5cm×5cm×0.1cm and a second aluminium test object (1cm×1cm×0.02cm). For all devices (n=7), a standard protocol was used (with individual changes device-depended on when required). The standard protocol consisted of left craniocaudal acquisition (28 kV, 56 mAs, filter Molybdenum, target Molybdenum, 50N compression all in manual acquisition without modulation). Additionally, we varied the mAs (from 12.5 to 140) and used the available modulation options and filter/target combinations. The images were analysed with the software called ATIA and the generated files were evaluated in a Microsoft Excel routine also provided by the IAEA. SNR, SDNR, MTF horizontal (20%), MTF vertical (20%) and d' (diameter D=0.1) were compared to characterize device performance with respect to the protocol doses (Mean Glandular Dose - MGD).

Results

For the standard protocol, the obtained SNR ranged from 33.52 to 128.68 for the tested devices. Additionally, 4.26 to 4.77, 3.39 to 7.05, 3.37 to 7.75 and 0,.1 to 0.75, respectively for SDNR, MTF hor (20%), MTF vert (20%) and d'. Within a single device, the largest variation of MGD observed was from 0.17 mGy to 9.27 mGy for the evaluated protocols (considering manual, semi and automatic mode).

Conclusion

The platform provided by the IAEA, including hardware and software, allows for preliminary characterization of mammography devices based on image quality metrics.

N-Peaks, a novel method of intensity normalization for magnetic resonance images

Author: Philipp Wallimann[1]

Co-authors: Hubert S. Gabrys[1], Janita E. Van Timmeren[1], Javier B. Garcia[1], Mariia Lapaeva[1,2], Zahra Khodabakhshi[1], Marta Bogowicz[1], Matthias Guckenberger[1], Nicolaus Andratschke[1], Stephanie Tanadini-Lang[1]

[1]*Department of Radiation Oncology, University Hospital Zurich, Zurich, Switzerland*

[2]*ETH Zürich, Zürich, Switzerland*

Purpose

Intensity units in magnetic resonance (MR) images have no inherent meaning. Quantitative evaluation of MR images may benefit from an intensity normalization. There exists no consensus about the best intensity normalization method, and most approaches do not consider physiological meaning of image regions or are restricted to specific body regions. We developed a novel approach for MR intensity normalization, called N-Peaks, which produces intensity units with a physiological connection while being applicable in any body region.

Methods

N-Peaks requires an image from any body region and an arbitrary number (N) of contours describing histologically different tissues. In each contour, it determines the peak of the homogeneous tissue in the intensity histogram and uses those peak intensities as landmarks for normalization to a target intensity scale. The homogeneous tissue in each contour is isolated by excluding voxels where the magnitude of local intensity change is higher than an automatically determined threshold. The remaining region should contain one or more intensity peaks, corresponding to different sub-regions, of which one peak is chosen. The result can be interpreted by visualizing the found homogeneous region and intensity peak. Finally, a piecewise linear intensity transformation is applied to the image such that peak intensities are mapped to target intensity values. We tested N-Peaks on 2308 brain MRI using four sequences (T1, T1c, T2 and FLAIR) from the Brain Tumor Segmentation challenge dataset using cerebrospinal fluid and white matter as contours. For each sequence, the intensity-volume histogram of brain tissue was determined for each image and the Jensen-Shannon distance (JSD) was calculated to the average histogram across all images in that sequence.

Results

The mean JSD (±1 standard deviation) for T1, T1c, T2 and FLAIR were: without normalization 0.55(±0.05), 0.54(±0.06), 0.31(±0.13) and 0.48(±0.08); and with N-Peaks 0.13(±0.03), 0.12(±0.04), 0.14(±0.03) and 0.18(±0.06).

Conclusion

N-Peaks is a flexible, physiologically motivated and interpretable MR intensity normalization technique. The improved consistency of the intensities was demonstrated in brain MRI in the form of lowered JSD values between histograms.

Practice of domain knowledge towards robust and generalizable deep learning-based CT-free PET attenuation and scatter correction

Author: Song Xue[1]

Co-authors: Rui Guo[2], Axel Rominger[3], Kuangyu Shi[3]

[1]*University of Bern, Bern, Switzerland*

[2]*Department of Nuclear Medicine, Ruijin Hospital, Shanghai Jiao Tong University School of Medicine, Shanghai, China*

[3]*Department of Nuclear Medicine, Inselspital, Bern University Hospital, University of Bern, Bern, Switzerland*

Purpose

Deep learning (DL)-based methods have been proposed to substitute CT-based PET attenuation and scatter correction to achieve CT-free PET imaging. A critical bottleneck for these DL-based methods is their limited capability in the application in the heterogeneous domain of PET imaging, i.e. a variety of scanners and tracers. This study employs a simple way to integrate domain knowledge in deep learning for CT-free PET imaging.

Materials and Methods

In contrast to conventional direct deep learning methods, we simplify the complex problem by a domain decomposition so that the learning of anatomy-dependent attenuation correction can be achieved robustly in a low-frequency domain while the original anatomy-independent high-frequency texture can be preserved during the processing. The effectiveness and robustness of our proposed approach was verified in tests of external imaging tracers on different scanners. Whole body PET images of 829 patients using 18F-FDG, 18F-PSMA, 68Ga-DOTA-TOC, 68Ga-DOTA-TATE, 68Ga-FAPI, acquired using clinical PET scanners, including Biograph Vision (Siemens Healthineers), United Imaging uMI 780 (United Imaging), Discovery MI (General Electric Healthcare) in Shanghai and Bern, were included for the development and testing of the proposed method.

Results

Although the method was developed using one tracer (18FFDG) and one scanner, it achieved an average whole-body normalized root mean squared error (NRMSE) and peak signal-to-noise ratio (PSNR) of 0.3%±0.2% and 51.5±6.4 respectively for different scanners, and 0.6%±0.4% and 47.5±7.4 for different tracers, which have significantly improved over conventional deep learning methods.

Conclusion

The proposed decomposition-based method provides a simple approach to incorporating domain knowledge in deep learning, which can significantly improve the performance and robustness of CT-free PET correction. The robust, generalizable and transparent DL development may enhance the potential of clinical translation.

Comparison of generative adversarial networks trained in paired and unpaired fashion for MR-based synthetic CT generation towards MR-only radiotherapy in the abdomen

Author: Mariia Lapaeva[1,2,3]

Co-authors: Agustina La Greca Saint-Esteven[1], Philipp Wallimann[1], Manuel Günther[2], Ender Konukoglu[3], Nicolaus Andratschke[1], Matthias Guckenberger[1], Stephanie Tanadini-Lang[1], Riccardo Dal Bello[1]

[1]*Department of Radiation Oncology, University Hospital Zurich and University of Zurich, Zurich, Switzerland*

[2]*Artificial Intelligence and Machine Learning Group, Department of Informatics, University of Zurich, Zurich, Switzerland*

[3]*Computer Vision Laboratory, ETH Zurich, Zurich, Switzerland*

Purpose

The aim of this study is to compare deep learning (DL) approaches trained on co-registered image pairs (paired data) and unpaired data requiring only images from each modality. The generation of synthetic CT (sCT) images from magnetic resonance (MR) images acquired with a TrueFISP sequence at a 0.35T hybrid MR-Linac is investigated along with their application for quality assurance (QA).

Materials and Methods

A retrospective analysis for 76 patients with a tumour in the abdomen treated at our institution was carried out. First, the influence of generative adversarial network (GAN) architectures trained in paired (Pix2pix) and unpaired fashion (CycleGAN; CUT) were assessed. Second, diverse pre-processing routines (N4 bias field correction; Nyul and novel N-Peaks intensity normalisations) were evaluated. Finally, two input-output network channels configurations (2D, pseudo3D) were compared. Both image similarity metrics and dose-volume histogram (DVH) indicators were used to assess the quality of the generated sCT.

Results

The mean absolute errors (mean ± SD) for best performing configurations are 71.0±20 HU for Pix2pix (Nyul, pseudo3D), 73.4±21 HU for CycleGAN (Nyul, 2D) and 84.5 ±19 HU for CUT (N4 and N-Peaks, 2D). Importantly, trained in unpaired fashion CycleGAN and CUT excel beyond Pix2pix and deformable registration methods in the air pockets reproduction. Regarding the DVH indicators, high correspondence in dose distribution is observed, with mean dose discrepancies below 1% for the planning tumour volume indicators of all models and Dmean equals to 0.33%, 0.32% and 0.40% for Pix2pix, CycleGAN and CUT.

Conclusion

Our study shows that unpaired-trained GANs achieve comparable performance to models requiring perfectly aligned image pairs, essential in the context of scarce clinical data. It also demonstrates that the application of unpaired-trained GANs affects positively the sCT quality for the abdominal region, characterised by significant differences in the shape and location of non-rigid organs and air pockets. The optimisation of various training configuration allows our models to outperform the current state-of-the-art, revealing their potential for clinical application and further implementation of QA procedures for MR-only radiotherapy.

Dosimetric and image quality comparison of radiation oncology and radiology head scan protocols

Author: Thiago Lima[1]

Co-authors: Paolo Zucchetti[1], Regina Seiler[1], Milena Cristina Gravinatti[1], Mirjam Heinrich[1], Justus Roos[1], Thomas Götzfried[1]

[1]*Luzerner Kantonsspital, Luzern, Switzerland*

Purpose

Imaging plays a more and more important role in radiation oncology (RO) treatments with technological advances and increased complexity of treatment techniques (hypofractionation, IGRT, SRT etc.). This study aimed to compare our RO head scan protocols with those present in our radiology (RA) department based on their radiation exposure and image quality.

Materials and Methods

The standard RO head CT scan protocol for treatment planning (PCT) and the head CBCT scan protocol for IGRT were compared with our RA native head scan protocol in addition to our preoperative protocols for the paranasal sinuses and the temporal bone. The devices covered in this study included an MSCT scanner Canon Aquilion and an on-board cone beam CT system at a TrueBeam linac (RO), and for RA, an MSCT scanner Siemens Definition Force and the CBCT scanner NewTom 5GXL. For the dosimetry, an Alderson phantom was used. Thermoluminescent dosimeters (TLD MCP-N, RaDPro) measured absorbed dose (mSv) at sensitive locations (eyes, nasal cavity, thyroid, brain). The mean value of a set of three dosimeters for each location was calculated. CatPhan 604-based images were analyzed using Pylinac scripts for the image quality aspect.

Results

Measured PCT in-field doses were all in the same range of 46±4 mSv except for the thyroid with a significantly higher value of 71 mSv. RO-CBCT doses were more than an order of magnitude lower. In comparison to the RA protocols, differences in dose were equivalent to the changes in protocol doses (~30% higher and ~60% lower for CT and CBCT, respectively, when comparing RO and RA protocols). Similar image quality (MTF, noise and low contrast detectability) was obtained by all the different devices with specific differences found.

Conclusion

RO-CBCT doses are configured in such a way that sufficient image quality is achieved. This ensures an acceptable total patient dose, even with frequent exposures, and allows, with high geometric fidelity, the position of the tumor and surrounding tissues along with organs at risk to be accurately identified.

Session IV: Radioprotection, Treatment Techniques

28.10.2022, 13:15 – 14:45

Chair: Francesca Belosi,
University Hospital of Zurich

Dosimetrically-motivated beam-angle optimization for partial-arc non-coplanar VMAT

Author: Chengchen Zhu[1]

Co-authors: Jenny Bertholet[1], Silvan Mueller[1], Gian Guyer[1], Paul-Henry Mackeprang[1], Hannes A. Loebner[1], Marco F. M. Stampanoni[2], Michael K. Fix[1], Peter Manser[1]

[1]*Division of Medical Radiation Physics and Department of Radiation Oncology, Inselspital, Bern University Hospital, and University of Bern, Bern, Switzerland*

[2]*Institute for Biomedical Engineering, ETH Zürich and PSI, Villigen, Switzerland*

Purpose

To develop a beam-angle optimization method for non-coplanar VMAT (NC-VMAT) with table-angle and gantry-angle range determined by iterative beam elimination based on 4-π fluence map optimization (FMO).

Materials and Methods

FMO is carried out for beam directions covering the 4-π space around the PTV every 10° gantry-angle and 10° table-angle. A gantry-table contribution map is generated from the fractional contribution of each beam to PTV dose. The map is thresholded to eliminate 25% of the beams with the lowest contribution. Pseudo-arcs are formed by adjacent beams with the same table-angle. Subsequently, FMO is applied to the remaining beams and pseudo-arcs are trimmed by eliminating the 25% lowest-contributing beams at the start and stop (edges) of all pseudo-arcs. Pseudo-arcs spanning less than 55° gantry-angle range are rejected. FMO, trimming, and small-arc rejection are repeated iteratively until reaching a user-defined total gantry-angle range. The resulting pseudo-arcs are converted into dynamic-arcs and subject to hybrid direct aperture optimization (HDAO), yielding a mechanically deliverable NC-VMAT plan. The method was applied to a clinically-motivated locally recurrent nasopharyngeal carcinoma case (NPC, 25x2 Gy). A HDAO-optimized coplanar-VMAT plan with the same total gantry-angle range was created for comparison.

Results

The desired total gantry-angle range of 720° was reached in 4 iterations yielding a NC-VMAT plan with seven partial-arcs with table angles between -40° and 60° and gantry-angle range from 60° to 130°. The cost function values after HDAO and dose re-normalization were 0.045 for NC-VMAT and 0.066 for coplanar-VMAT. Target coverage was similar for both techniques. Dmax to optic nerves, lenses, optic chiasm, brainstem PRV, and spinal cord PRV were 0.7-6.2 Gy lower for NC-VMAT than for coplanar-VMAT.

Conclusion

A dosimetrically-motivated beam-angle optimization method was developed using iterative 4-π FMO and beam elimination. A NC-VMAT plan was optimized for an NPC case using HDAO to obtain a mechanically deliverable plan achieving better OAR-sparing than coplanar-VMAT.

Disclosures

This work was partially supported by Varian Medical Systems and by grant 20021_185366 of the Swiss National Science Foundation.

Involvement of medical physicists in medical practices operating a fluoroscopy system

Author: Reto Treier[1]

Co-authors: Philipp R. Trueb[1]

[1]*Federal Office of Public Health, Bern, Switzerland*

Purpose

According to Article 36 of the Radiological Protection Ordinance, medical physicists must be involved in fluoroscopy in the medium- and high-dose range (i.e. examinations resulting in effective doses for the patients > 1 mSv). While the involvement has become well established in hospitals and radiological institutes, the situation in medical practices operating a fluoroscopy system is unclear. Therefore, the Federal Office of Public Health conducted a survey to assess the indications and to determine the dose ranges of the fluoroscopy-based procedures in the medical practices.

Methods

Between June and August 2021, information from 103 medical practices operating a fluoroscopy system was collected. The information contained details on the indications, the body/organ regions examined and the dose area product (DAP) and duration of fluoroscopy of at least three of the most recently performed procedures per indication. To estimate the effective dose, the DAP was multiplied by a conversion coefficient provided on the IAEA website and in ICRP publication No. 117. Results are presented as median (interquartile range).

Results

In most of the medical practices (85), fluoroscopy is used in pain therapy, followed by interventions in gastroenterology (9), urology (6), angiology (2) and cardiology (1). DAP and duration of fluoroscopy are in pain therapy of spine/pelvis/hip 0.10 (0.04-0.24) mSv and 19 (8-39) s; for cystography 0.27 (0.12-0.47) mSv and 29 (11-35) s; for nephrostomy 0.44 (0.11-0.66) mSv and 38 (13-78) s; for dilatation of esophagus 1.35 (1.19-1.86) mSv and 175 (158-280) s; for dilatations in the abdomen 0.59 (0.47-0.76) mSv and 330 (171-426) s; for PTA in pelvis/leg 2.78 (1.02-4.42) mSv and 525 (246-656) s. For coronary angiography, only three datasets were collected: 8.58 mSv and 180 s, 1.66 mSv and 291 s, 6.07 mSv and 174 s.

Conclusion

In pain therapy, the involvement of medical physicists is not legally required, for gastroenterological and urological procedures, it should be assessed individually and for angiological and cardiological procedures, it is mandatory.

Monitoring of medical population dose in Switzerland – How to move forward

Author: Barbara Ott[1]

Co-authors: Boris Kaiser[2], Florentin Krämer[2], Philipp R. Trueb[1]

[1]*Federal Office of Public Health, Bern, Switzerland*

[2]*BSS Volkswirtschaftliche Beratung, Basel, Switzerland*

Purpose

Imaging procedures are indispensable for diagnostics and patient treatment, but they also involve health risks due to the use of ionising radiation. Therefore, the FOPH monitors the radiation exposure of the Swiss population. The frequency of diagnostic examinations performed is recorded and the mean effective dose is estimated. This monitoring helps to recognize emerging changes and trends at an early stage. Due to the digitalisation in medicine, the data required for the monitoring is now partly available in electronic form. This work demonstrates the feasibility of future automation.

Materials and Methods

Possible data sources for the collection of the frequency of the different modalities are identified, their coverage is reported, automated access to the data is demonstrated and the connection to the previous surveys assured. The results are used to propose an update on the CT population dose for the period 2018-2020.

Results

Relevant data sources are available that allow to estimate the frequencies of the different examinations. Modalities used and anatomical regions examined can be derived from billing or classification codes: TARMED for outpatients, Swiss surgical classification (CHOP) for inpatients. Retrospective calculation of the frequencies up to and including 2013 allow the linkage to the previous monitoring. Initial estimations carried out for selected modalities show comparable trends.

Conclusions

The periodic survey of medical radiation frequencies in Switzerland is feasible for some modalities. A major advantage of this method is the use of existing data sources, which will enable publishing results at shorter intervals. The data sources allow for evaluations by canton or large region, age group and gender. Furthermore, analyses according to service provider characteristics, such as a breakdown by practices and hospitals, are possible. Certain limitations result from the nature of the data used. Only billed activity examinations are recorded. They do not necessarily correspond to the examinations actually carried out.

Disclosures

BSS received funding from BAG for its work.

Proposed DRLs for mammography in Switzerland

Author: Laura Dupont[1]

Co-authors: Christoph Aberle[2], Marta S. Merce[1], Alexander Schegerer[3], Diomedis Botsikas[1], Michael Ith[4], Thiago Lima[5], Roman Menz[2], Pascal Monnin[6], Stefano Presilla[7], Philipp Trueb[8]

[1]*Geneva University Hospital, Geneva, Switzerland*

[2]*Basel University Hospital, Basel, Switzerland*

[3]*Hirslanden Clinic, Zürich, Switzerland*

[4]*Inselspital, Bern, Switzerland*

[5]*Lucerne Cantonal Hospital, Lucerne, Switzerland*

[6]*Vaud University Hospital Centre, Lausanne, Switzerland*

[7]*Lugano Regional Hospital, Lugano, Switzerland*

[8]*Federal Office of Public Health, Bern, Switzerland*

Purpose

The aim of this study is to propose Diagnostic Reference Levels (DRLs) values for Mammography in Switzerland.

Materials and Methods

The data was obtained by means of a survey. A total of 31 centres including 5 University hospitals, several cantonal hospitals, and large private clinics, globally covering all linguistic regions of Switzerland participated in the data collection. The data gathered contained all the necessary technical information: manufacturer and model of the device, kV, mAs, mean glandular dose (MGD), etc. The data collected was considered to be representative of the practice in Switzerland.

Results

From the 31 institutes contacted, information was received from 36 mammography units (6 different manufacturers represented) and 24762 acquisitions. For most of the centres, the data was extracted from the dose management system (DMS). Those not having their mammography unit connected to a DMS weren't keen to participate. The data collected was sorted into the following categories: 2D projection or 3D digital breast tomosynthesis (DBT) examination, craniocaudal (CC) or mediolateral oblique (MLO) projection, and 8 different categories of compressed breast thickness (CBT) ranging from 20mm to 100mm in 10mm width intervals. The analysis showed that the data obtained reflects of the practice in Switzerland, and the most frequently used units are represented in this study. The main results revealed that the MGD is larger for 3D than for 2D acquisitions for the same CBT. When the CBT increased from 20mm to 100mm, the 75th percentile of the MGD values obtained increased from 0.81mGy to 2.96mGy for 2D examinations, and from 1.22mGy to 4.04mGy for 3D examinations, for both projections (CC/MLO). The results obtained were compared with the DRLs values of several other countries for similar methodologies and are in good agreement.

Conclusion

Swiss diagnostic reference values (DRLs) can be proposed according to the examination type (2D/3D), projection (CC/MLO) and CBT. The proposed values compare well with those obtained in the literature that have been performed using the same methodology.

Kerma - effective dose factor of the eye of pediatric patient during intra-arterial chemotherapy

Author: Marion Dercourt[1]

Co-authors: Lucia G. Manzano[1], Marie Nowak[1]

[1]*CHUV – Centre Hospitalier Universitaire Vaudois, Lausanne, Switzerland*

Purpose

Retinoblastoma is a rare eye tumor that develops in children up to 4 years old. Intra-arterial chemotherapy (IAC) is an emerging treatment modality that is gaining recognition worldwide. IAC requires fluoroscopy assistance, which involves multiple irradiations. As consequence, children undergoing IAC can sustain damage to eye lens such as cataracts and radiation induced cancer. The aim of the project was to find correction factors between the air Kerma at the reference point and the eye lens dose.

Materials and Methods

Retinoblastoma procedures performed between May 2021 and June 2022 with C-arm system (Philips Allura-Xper, FD20/20) were reviewed. Patient's characteristics (age, sex, head size) and radiation exposure parameters (Kerma, table height) were collected. Effective doses were measured using thermoluminescent detectors (TLD) placed on both eyes and temples. For this study, two correction factors were calculated: the ratio of the effective dose (ED) measured by the TLDs to the total Kerma (Ktot) found on the dose report, and the ratio of the ED to the corrected Kerma (Kcor), which takes into account the table height and patient's thickness.

Results

The study included 23 retinoblastoma procedures in 20 patients. The median ratio between the dose to the right and left eyes and Ktot was 0.12 and 0.33, respectively, whilst the ratio of Kcor was 0.22 and 0.53. The correction factor using Kcor is respectively 83% and 60% higher than that of Ktot. In addition, results show that the median ED is 1.96 times higher for the left eye than for the right eye.

Conclusion

This study shows the existing bias between the dose estimated from Ktot and the Kerma at the eye level. The right and left eye doses can now be estimated directly from the Kerma obtained either on the dose report, or more accurately, from the radiation dose structured report. In addition, results highlight that the left eye receives two times more dose than the right eye due to the machine configuration. This could be optimized with a biplane tube changing sides.

On an auto-commissioning for an electron beam model applicable to MLC collimated electron beams

Author: Silvan Mueller[1]

Co-authors: Michael K. Fix[1], Daniel Frei[1], Gian Guyer[1], Hannes A. Loebner[1], Werner Volken[1], Peter Manser[1]

[1]Division of Medical Radiation Physics and Department of Radiation Oncology, Inselspital, Bern University Hospital, and University of Bern, Bern, Switzerland

Purpose

Using the photon multileaf collimator (MLC) instead of the electron applicator is a promising solution to improve clinical workflow and enable intensity modulation for electron radiotherapy. Currently, an inefficient manual process is performed to commission beam models for MLC shaped electron beams. The aim of this work is to develop an auto-commissioning procedure for a Monte Carlo (MC) electron beam model of TrueBeam systems.

Materials and Methods

The beam model includes two sources each consisting of an electron and a photon part: a main source representing the primary beam and a jaw source representing the head scatter contribution. For the particle transport through the MLC, MC simulation is performed. The commissioning procedure uses pre-determined information from BEAMnrc and electron MC (eMC) simulations and in total seven measurement scans in air and water to automatically determine the fluence distributions, weights, energy spectra and focal spot position and lateral intensity distribution of the beam model sources. For validation purposes, calculated and measured dose distributions in water were compared for different field sizes (2x2-10x10 cm2), source to surface distances (SSDs) (70-100 cm) and beam energies (6-22 MeV) for eight TrueBeam systems of six different institutions, either equipped with a Millennium 120 MLC or with a high-definition MLC. Furthermore, calculated and film measured dose distributions of a single electron field plan for a sternum case in an anthropomorphic phantom were compared at different SSDs.

Results

The auto-commissioning procedure was successfully applied to eight TrueBeam systems in minutes instead of several days that were necessary for the manual commissioning. Measured and calculated dose distributions agree generally within 3% of maximum dose or 2 mm. Gamma passing rates for the sternum case using 3% (global) / 2 mm criteria with a threshold of 10% ranged from 96% to 99% for different SSDs.

Conclusions

The developed auto-commissioning procedure enables an efficient commissioning of an MC electron beam model and simplifies the usage of MLC shaped electron beams.

Disclosures

This work was partially supported by Varian Medical Systems.

Dosimetric comparison between modulated electron radiotherapy, mixed beam radiotherapy and volumetric modulated arc therapy

Author: Anne H. zur Horst[1]

Co-authors: Gian Guyer[1], Silvan Mueller[1], Werner Volken[1], Daniel M. Aebersold[1], Marco F. M. Stampanoni[2], Michael K. Fix[1], Peter Manser[1]

[1]*Division of Medical Radiation Physics and Department of Radiation Oncology, Inselspital, Bern University Hospital, and University of Bern, Bern, Switzerland*

[2]*Institute for Biomedical Engineering, ETH Zürich and PSI, Villigen, Switzerland*

Purpose

Treatment plans with photon beams typically rely on photon multi-leaf collimators (pMLC) in clinical routine which enable techniques such as volumetric modulated arc therapy (VMAT). Intensity and energy modulated electron beams are facilitated by the usage of pMLCs instead of cut-outs in so-called electron modulated arc therapy (EMAT) and modulated electron radiotherapy (MERT). In mixed beam radiotherapy (MBRT), intensity modulated photon and electron beams are combined. In this work, EMAT, MERT and MBRT plans are compared to VMAT plans.

Materials and Methods

EMAT, MERT, VMAT, and MBRT plans are created for two breast cases and three head and neck (H&N) cases. For this, electron arcs, electron fields and photon arcs are set up within a treatment planning system and intensity modulation optimisation is performed using an in-house optimizer. The treatment plan quality of the created EMAT, MERT, VMAT and MBRT plans is assessed via dose-volume histograms, dose distributions and dose statistics. The dosimetric accuracy is validated with radiochromic film measurements for a selection of plans.

Results

For the investigated breast cases, the generated MERT/EMAT plans show an improved treatment plan quality compared to VMAT plans. For the H&N cases, however, the VMAT plans outperformed the MERT/EMAT plans in terms of treatment plan quality. Overall, the results for the MERT plans are similar to the EMAT plans in terms of their dose distributions. Further, the treatment plan quality is improved using MBRT in comparison to MERT/EMAT/VMAT plans. The gamma passing rate between measured and calculated dose distributions are above 97.1% for all investigated plans using a 3%(global)/2mm criterion.

Conclusions

The generated MERT and EMAT plans are similar in terms of dosimetric treatment plan quality. In comparison to VMAT, the EMAT and MERT plans have improved treatment plan quality for the breast cases, but worse treatment plan quality for the H&N cases, while the MBRT plans achieved best treatment plan quality overall.

Disclosures

This work was partially supported by grant 200021_185366 of the Swiss National Science Foundation and by Varian Medical Systems.

Role of proton beam angle flexibility for combined proton-photon therapy of head and neck cancer

Author: Florian Amstuz[1]

Co-authors: Reinhardt Krcek[1], Barbara Bachtiary[1], Damian C. Weber[1], Antony J. Lomax[1], Jan Unkelbach[2], Ye Zhang[1]

[1]*PSI – Paul Scherrer Institute, Villigen, Switzerland*

[2]*University Hospital Zürich, Zürich, Switzerland*

Purpose

Optimally combined proton-photon therapy (CPPT) delivered with a fixed horizontal proton beamline (FHB) and a photon linac showed to be a promising option to increase access to proton therapy for head and neck (HN), breast and lung cancer (Fabiano 2020, Marc 2022, Amstutz 2022). Here, the investigation for HN cancer extends to explore the dependence of CPPT on the flexibility of proton beam angles and the impact of anatomical changes.

Materials and Methods

For a HN cancer patient with one planning CT and seven repeated CTs (repCTs) multiple treatment plans were optimized: a) IMRT (19 fields), b) IMPT-FHB (4 horizontal fields) c) IMPT-Gantry (3 gantry fields), d) IMPT-"arc" (19 gantry fields), e) CPPT-FHB (fields a&b), f) CPPT-Gantry (fields a&c), g) CPPT-"arc" (fields a&d). The CPPT gantry and "arc" plans are going beyond the motivation of increasing access to proton therapy and investigate the plan quality boundaries of CPPT. A non-adaptive (recalculations on repCTs) and an adaptive regime (replanning on repCTs) were investigated for each plan. Plans were evaluated visually, with DVHs, and with dose parameters. NTCPs for Xerostomia and Dysphagia of grade ≥2 were calculated for all plans (Langendijk 2021).

Results

Adaption showed to be necessary for all treatment plans to keep a high target coverage. The trend for the NTCPs are the same for both side effects. The CPPT improves plan quality compared to its IMPT counterparts, e.g. Xerostomia: FHB (24.6% vs. 30.3%), gantry (23.7% vs. 24.4%) and "Arc" (22.5% vs. 23.3%), and compared to IMRT (27.1%). Additionally, plan quality increases with more flexible proton beam angles. In parallel, the proton component increases, with the contribution from protons to the mean PTV dose being: FHB 77%, gantry 87%, "arc" 99%.

Conclusion

Extending proton beam angles flexibility increases plan quality for CPPT. Meanwhile, the proton component of CPPT gets more dominant. However, the photon component can still increase the quality for each level of beam angle flexibility. Further investigations are needed to find the optimum between flexibility (costs) and plan quality.

An ultra-fast field delivery with PSI's Gantry-2 to achieve hypofractionated PBS proton therapy within a single breath-hold for lung cancer

Author: Vivek Maradia[1]

Co-authors: Steven Van De Water[2], David Meer[1], Damian Charles Weber[1], Antony John Lomax[1], Serena Psoroulas[1]

[1]*PSI – Paul Scherrer Institute, Villigen, Switzerland*

[2]*Department of Radiation Oncology, Amsterdam UMC, Vrije Universiteit Amsterdam, Cancer Center Amsterdam, Amsterdam, The Netherlands*

Purpose

The use of motion mitigation techniques such as breath-hold can reduce the dosimetric uncertainty of lung cancer proton therapy. We studied the feasibility of hypofractionated pencil beam scanning (PBS) proton therapy field delivery within a single breath-hold at PSI's Gantry 2. Treatment delivery time in PBS proton therapy depends on beam-on time and the dead time between proton spots (time required to change the energy and/or lateral spot position). We studied ways to reduce beam-on and lateral scanning time, without sacrificing dosimetric plan quality, aiming at a single field delivery time of 15 seconds at maximum. We tested this approach on ten lung cancer cases with varying target volumes (PTV volume range 137-379 cm3).

Methods

To reduce the beam-on time, we increased the beam current at the isocenter by developing new beam optics for PSI's PROSCAN beamline and Gantry 2. Experimentally we obtained up to factor 5 higher transmission for all proton energies. To reduce the dead time between the spots, we used spot-reduced plan optimization. First, a 3-field SFUD treatment plan was generated for all 10 cases using the in-house clinical planning system 'PSIplan'. Spot-reduced plans were subsequently generated while mimicking relevant dosimetric plan parameters of the clinical plans to ensure comparable plan quality. The spot reduction technique reduced the number of spots by 95% compared with the clinical planning system for the lung cases considered. For the clinical and spot-reduced plans, 6-Gy(RBE) fractions were delivered with PSI's Gantry 2 using the clinical and transmission-efficient beam optics, respectively. We extracted delivery times, including both beam-on time and dead time, from the log files.

Results

We found that it is possible to achieve hypofractionated (6 Gy(RBE)/fraction) field delivery times within a single breath-hold (6 Gy(RBE)/fraction) field delivery times within a single breath-hold (<15 sec) for all (100%) index cases.

Conclusions

In summary, the combination of spot reduction and improved beamline transmission is a promising approach for treating mobile tumors treated with PBS proton therapy within clinically achievable breath-hold durations.

VERIQA

PTW THE DOSIMETRY COMPANY

The Modular Software Platform for Comprehensive Patient QA

One platform. Flexible and scalable.

From visualization and evaluation to verification and reporting, VERIQA is an all in one software built on future-proof client-server architecture.

Automated workflows. Streamlined operations.

Take your workflow efficiency to the next level by automating your patient-specific quality.

Track. Trend. Monitor.

Track and analyze your results with the automated integration of Track-it.

Automated plan verification

VERIQA gives you the choice to select the best method for specific verification needs – from independent dose calculations, pre-treatment and in vivo EPID dosimetry over log file analysis to phantom-based measurements with OCTAVIUS® 4D.

Monte Carlo dose calculations: Fast and precise.

VERIQA calculates dose using the well-established SciMoCa™ Monte Carlo algorithm known for its accuracy and reliability. Use this gold standard method to automatically evaluate your treatment plans in 3D with minimum effort.

Advanced 3D EPID dosimetry

Based on a clinically proven algorithm enhanced with a unique, patent-pending Monte Carlo-based inhomogeneity correction, VERIQA RT EPID 3D is the new Patient QA module to come for true 3D pre-treatment and in vivo EPID dosimetry.

ptwveriqa.com

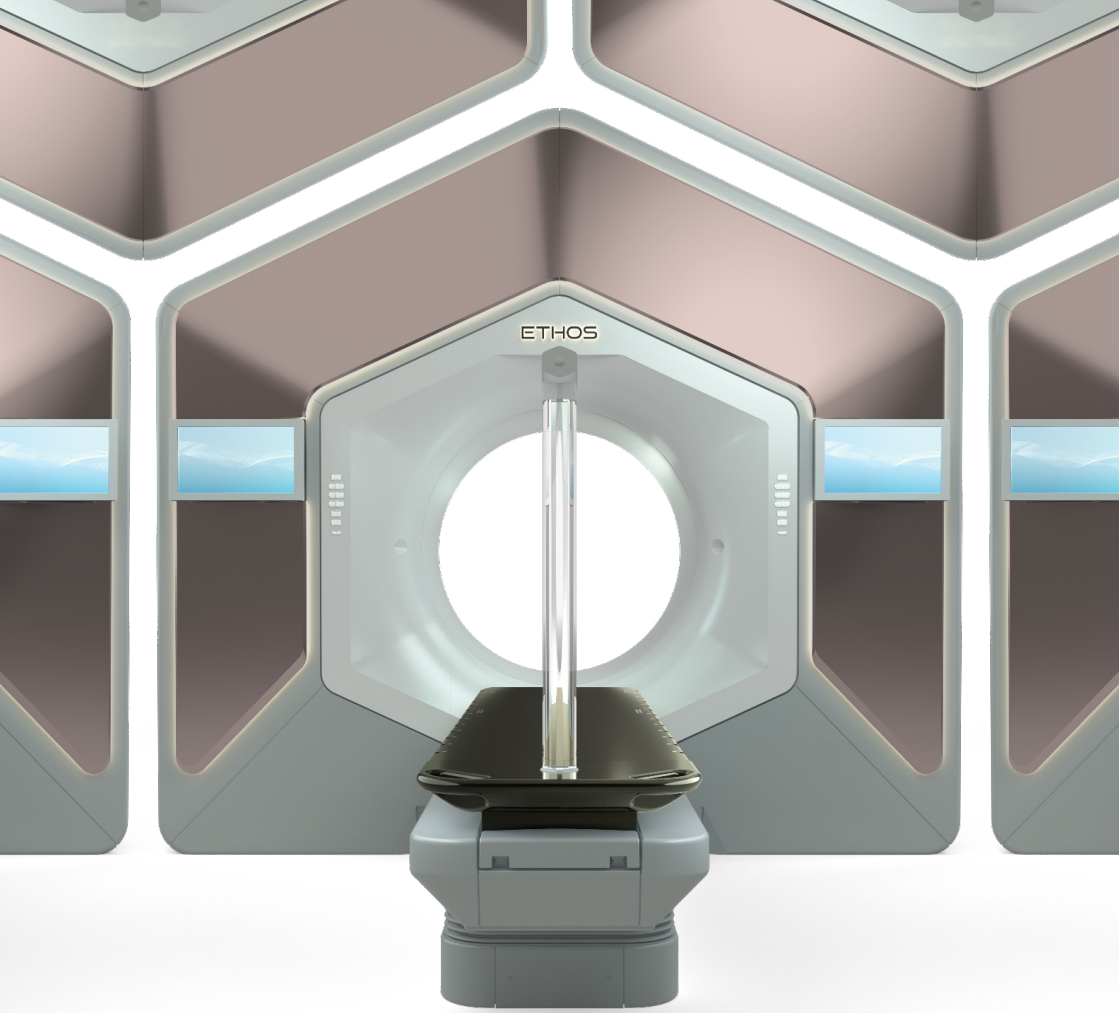

The more efficient, flexible, personal

& intelligent way to outsmart cancer.

With Ethos™ therapy, you can adapt treatment plans daily while transforming your cancer fight completely.

Ethos therapy is our AI-driven holistic solution that lets you choose the most appropriate treatment option based on daily changes in patient anatomy. It also delivers an entire adaptive treatment in a typical 15-minute timeslot, from setup through delivery. Redefine how you fight cancer—experience Ethos therapy at varian.com/ethos today.

Safety Information: Radiation may cause side effects and may not be appropriate for all cancers.

varian
A Siemens Healthineers Company

ETHOS™